

Ricardo Arruda Monteiro da Silva
Laboratório de Dinâmica e Modelagem Oceânica (DinaMO)

Fluxos de CO_2 entre oceano e atmosfera
e os controladores da variabilidade de
 pCO_2 superficial no oceano Atlântico
Sudoeste

Rio Grande
2015

Ricardo Arruda Monteiro da Silva
Laboratório de Dinâmica e Modelagem Oceânica (DinaMO)

Fluxos de CO_2 entre oceano e atmosfera
e os controladores da variabilidade de
 pCO_2 superficial no oceano Atlântico
Sudoeste

Dissertação apresentada ao Instituto de
Oceanografia da Universidade Federal do
Rio Grande, para a obtencao do título de
Mestre em Oceanografia Física, Química e
Geológica.

Orientador: Paulo Henrique Rezende Calil

Rio Grande
2015

Ricardo Arruda Monteiro da Silva.

Fluxos de CO_2 entre oceano e atmosfera
e os controladores da variabilidade de
 pCO_2 superficial no oceano Atlântico Sudoeste

68 páginas

Dissertação (Mestrado) - Instituto de Oceanografia, Universidade federal do Rio Grande.

1. Fluxo líquido de CO_2

2. pCO_2

3. Biogeoquímica marinha

I. Instituto de Oceanografia, Universidade federal do Rio Grande.

Comissão Julgadora:

Prof. Dr.

Alejandro A. Bianchi

Prof. Dr.

Rodrigo Kerr

Orientador - Prof. Dr.

Paulo H. R. Calil

Aos meus pais, Carlos Vollet Monteiro da Silva e Eliane Arruda Monteiro da Silva.

Epígrafe

"The fact that we live at the bottom of a deep gravity well,
on the surface of a gas covered planet going around a nuclear fireball
90 million miles away and think this to be normal is obviously
some indication of how skewed our perspective tends to be."

Don't Panic.

Douglas Adams, The Hitchhiker's Guide to the Galaxy.

Agradecimentos

Primeiramente gostaria de agradecer ao meu orientador, Paulo Calil, por todo o conhecimento passado, pela ajuda e pela prestatividade durante todo o mestrado. Agradeço também aos co-autores do manuscrito, Alejandro Bianchi, Scott Doney, Nicolas Gruber, Ivan Lima e Giuliana Turi pelas inúmeras correções, sugestões e discussões que ajudaram muito durante a elaboração do manuscrito, e novamente agradeço a Paulo Calil por ter possibilitado e incentivado esta grande colaboração de especialistas para o nosso trabalho. Agradeço aos membros da banca, Alejandro Bianchi e Rodrigo Kerr pela disponibilidade em participar da avaliação deste trabalho.

Agradeço à bolsa de mestrado concedida pela CAPES e ao Programa de Pós Graduação em Oceanografia Física, Química e Geológica, pelo apoio durante todo o curso, em especial durante a participação nos cursos de verão em Buenos Aires ("biogeochemical cycles") e em Xangai ("climeco4"), agradeço também o apoio de SCOR, CLIVAR e IMBER para a participação nesses cursos.

Agradeço ao apoio e companheirismo de todos os integrantes do Laboratório de Dinâmica e Modelagem Oceânica (DinaMO) e aos amigos do Cassinão. Por fim, agradeço aos meus pais que sempre me apoiaram desde o início de meus estudos.

Este trabalho foi financiado pelos seguintes projetos: Processos de Submesoescala e Consequências Biogeoquímicas (CNPq - 48312/2012-7), Bomba de Carbono na Plataforma Continental (FAPERGS - 2166/12-8) e Rede de Estudos da Corrente do Brasil na Margem Continental Sudeste-Sul - REMARSUL (CAPES 23038.004299/2014-53).

Resumo

Neste estudo foi utilizado um modelo biogeoquímico acoplado ao modelo físico ROMS para investigar as principais variáveis e processos responsáveis pela variabilidade espaço-temporal da pressão parcial do dióxido de carbono ($p\text{CO}_2$) e dos fluxos líquidos de CO_2 na interface oceano-atmosfera no oceano Atlântico Sudoeste. No geral, esta região se comporta como um sumidouro de CO_2 atmosférico ao Sul de 30°S , e se encontra próxima ao equilíbrio com a atmosfera ao Norte. Nas plataformas internas, o oceano atua como uma fraca fonte de CO_2 para a atmosfera. Já nas plataformas médias e externas, especialmente na Patagônia, o oceano atua como um sumidouro de CO_2 atmosférico. Os gradientes observados de $p\text{CO}_2$, tanto meridionais, quanto das plataformas internas para as externas, foram bem representados pela simulação. Uma análise de sensibilidade foi realizada e mostra a importância dos efeitos contrários da temperatura e da concentração de carbono inorgânico dissolvido (*DIC*) na regulação da variabilidade sazonal do $p\text{CO}_2$. Os processos mais importantes no controle da variabilidade de $p\text{CO}_2$ foram os processos de produção biológica e solubilidade do CO_2 , sendo que a produção biológica apresentou maior influência nas plataformas continentais. O papel da estratificação e mistura apresentou também importância na regulação das concentrações de *DIC* superficiais e consequentemente na regulação do $p\text{CO}_2$. Para exemplificar o papel da mistura, foi apresentado um perfil vertical no ponto ($42^\circ\text{S}, 42^\circ\text{W}$), onde será um ponto de monitoramento de variáveis físicas e biogeoquímicas do *Ocean Observatories Initiative* (OOI). Este trabalho está dividido em capítulos, no capítulo 1 é apresentado uma introdução com uma explanação geral do ciclo do carbono no ambiente marinho, apresentação da área de estudo, objetivos e motivação. No capítulo 2 é apresentado um detalhamento do modelo e dos métodos utilizados. No capítulo 3 está o manuscrito redigido na língua inglesa e submetido para a revista Biogeosciences, e por fim no capítulo 4 as considerações finais do estudo são apresentadas.

Palavras-chave: Fluxo líquido de CO_2 , $p\text{CO}_2$, biogeoquímica marinha

Listas de Figuras

| | |
|---|----|
| 1.1 Representação da área de estudo (retângulo vermelho) e das correntes superficiais do giro subtropical do oceano Atlântico Sul, adaptado de Peterson and Stramma (1991). | 21 |
| 2.1 Diagrama do modelo NPZD representando as fontes e os sumidouros para cada módulo biogeoquímico, adaptado de Gruber et al. (2006). | 25 |
| 3.1 Areas utilised for the temporal analysis, (a) show the 3 continental shelves (SEBS, SBS and PS) analysed in a map with annual mean ocean surface pCO_2 , the green circle represents the location of the vertical profile at the OOI site. (b) show the two oceanic regions (ST and SA) in a map with bathymetry. | 37 |
| 3.2 Seasonal climatology of modeled surface ocean pCO_2 (first row) and observations of pCO_2 from the SOCAT database (second row). The white separation between red and blue is set to $370 \mu atm$ which is the atmospheric pCO_2 used in this study. Blue represent a sink of atmospheric CO_2 and red a source. | 38 |
| 3.3 Model evaluation on the PS (zoom in from model domain in Fig. 2a). Seasonal climatology of modelled surface ocean pCO_2 (first row) and pCO_2 observations from ARGAU and GEF3 cruises(second row) (Bianchi et al., 2009). The white separation between red and blue is set to $370 \mu atm$ which is the atmospheric pCO_2 used in this study. Blue represent a sink of atmospheric CO_2 and red a source. | 39 |

| | | |
|------|--|----|
| 3.4 | Location of the three areas used for the monthly comparison with SOCAT database (a) in a map with annual averaged eddy kinetic energy. In figures (b), (c) and (d), green lines are the modelled monthly mean pCO_2 and black lines are the monthly mean pCO_2 from SOCAT. Error bars are two standard deviations | 40 |
| 3.5 | pCO_2 spatial anomalies - difference between annual mean and domain mean (a) and the contribution of the main drivers: ALK^s (b), FW (c), T (d) and DIC^s (e). Computed using spatial anomalies for Δ | 42 |
| 3.6 | Processes driving the annual mean surface pCO_2 . Contribution of Air-sea flux of CO_2 [Control - E1] (a), CO_2 solubility [E2 - E3] (b), physical transport [E3] (c) and biological production [E1 - E2] (d) | 43 |
| 3.7 | Sensitivity of pCO_2 computed with grid point anomalies in time to local annual means. Annual average contribution of the main drivers: ALK^s (a), T (b) and DIC^s (c). | 44 |
| 3.8 | Temporal evolution of pCO_2 anomalies and their drivers in each continental shelf (right hand side of Eq. 1 using monthly anomalies), red line represents the effects of Temperature, blue line the effects of DIC^s , green line FW, and yellow line ALK^s | 45 |
| 3.9 | temporal evolution of the monthly anomalies of each process in regulating pCO_2 anomalies, green line represents the biological production, red line the physical transport, light blue line the air-sea CO_2 fluxes and dark blue line the solubility. Black lines represent the temporal pCO_2 anomalies. | 48 |
| 3.10 | Figures (a) and (b) show the temporal evolution of pCO_2 anomalies and its drivers in each oceanic regions (ST and SA) (right hand side of Eq. 1 using monthly anomalies), red line represents the effects of T , blue line the effects of DIC^s , green line the FW and yellow line ALK^s . Figures (c), and (e) show the temporal evolution of the monthly anomalies of each process in regulating temporal pCO_2 anomalies, green line represents the biological production, red line the physical transport, light blue line the air-sea CO_2 fluxes and dark blue line the solubility. Black lines represent the temporal pCO_2 anomalies. | 49 |
| 3.11 | Figure (a) is the annual average of air-sea CO_2 fluxes. Figures (b), (c) and (d) show the monthly average of surface CO_2 fluxes constrained to bathymetry levels of 100m, 200m and 1000m. | 51 |

| | |
|---|----|
| 3.12 Vertical profile at 42° S, 42°W , upper panels showing monthly mean surface $p\text{CO}_2$ (solid black line), $p\text{CO}_2$ anomalies (dashed black line) and the contribution from the main drivers (Fig. (a) and (b)) and the main processes (Fig. (c). Lower panels showing vertical profiles of DIC (a), T (b), and chlorophyll concentration (c), black line represents the mixed layer depth. | 53 |
| 3.13 Seasonal climatology of modeled sea surface temperature $^{\circ}\text{C}$ - 4 years average (first row), and climatology from AVHRR sensor - from 1985 to 2002 (second row). | 56 |
| 3.14 Seasonal climatology of modeled chlorophyll-a concentration $\text{mgChla} - \text{am}^{-3}$ - 4 years average (first row), and climatology from Aqua-Modis sensor - from 2003 to 2013 (second row). | 57 |

Listas de Tabelas

| | | |
|-----|---|----|
| 2.1 | Detalhe dos experimentos para estimativa do efeito dos processos na variabilidade do $p\text{CO}_2$ (Turi et al., 2014) | 28 |
| 3.1 | Parameters of the biogeochemical model as in Gruber et al. (2006) | 34 |
| 3.2 | Statistic indicators of the model skill in the three areas (A1, A2 and A3 - Fig.3.4). Bold values indicate “good/excellent”or “reasonable”model skill when comparing to the SOCAT database. | 41 |

Listade Abreviaturas e Siglas

| | |
|----------|--|
| <i>S</i> | Salinidade |
| <i>T</i> | Temperatura |
| ALK | Alcalinidade Total |
| BC | Brazil Current |
| CESM | Community Earth System Model |
| CF | Cost Function |
| COADS | Comprehensive Ocean-Atmosphere Data Set |
| DIC | Carbono Inorgânico Dissolvido |
| E1 | Experimento 1 |
| E2 | Experimento 2 |
| E3 | Experimento 3 |
| FW | Fresh Water Flux |
| MC | Malvinas Current |
| ME | Modeling Eficiency |
| NPZD | Nitrogênio, Fitoplâncton, Zooplâncton e Detritos |
| OOI | Ocean Observatories Initiative |
| PAR | Photosynthetically Available Radiation |

| | |
|-------|-------------------------------------|
| PB | Percentage of Bias |
| PS | Patagonia Shelf |
| ROMS | Regional Ocean Modeling System |
| SA | Subantarctic oceanic region |
| SBS | South Brazilian Shelf |
| SEBS | Southeast Brazilian Shelf |
| SOCAT | Surface Ocean CO ₂ Atlas |
| SODA | Simple Ocean Data Assimilation |
| ST | Subtropical oceanic region |

Sumário

| | | |
|----------|--|-----------|
| 1 | Introdução | 15 |
| 1.1 | Ciclo do Carbono no ambiente marinho | 15 |
| 1.1.1 | Fluxos líquidos de CO ₂ na interface oceano-atmosfera | 17 |
| 1.1.2 | Papel das plataformas continentais | 18 |
| 1.2 | Área de Estudo e antecedentes | 20 |
| 1.3 | Objetivos | 21 |
| 1.4 | Motivação | 22 |
| 2 | Métodos | 24 |
| 2.1 | Modelo | 24 |
| 2.2 | Análises | 26 |
| 2.2.1 | Cálculo <i>pCO</i> ₂ | 26 |
| 2.2.2 | Estatísticas para avaliação do modelo | 26 |
| 2.2.3 | Cálculo dos Controladores | 27 |
| 2.2.4 | Estimativa dos processos reguladores | 28 |
| 3 | Manuscrito | 29 |
| 3.1 | Introduction | 31 |
| 3.2 | Materials and Methods | 33 |
| 3.2.1 | Model | 33 |
| 3.2.2 | Analysis | 34 |
| 3.3 | Model Evaluation and Validation | 37 |
| 3.4 | Results and Discussion | 41 |

| | | |
|----------|---|-----------|
| 3.4.1 | <i>pCO₂</i> drivers - spatial analysis | 41 |
| 3.4.2 | <i>pCO₂</i> drivers - temporal analysis | 44 |
| 3.4.3 | Air-sea <i>CO₂</i> fluxes | 50 |
| 3.4.4 | Vertical Structure - Case Study at Argentine OOI Site | 52 |
| 3.5 | Conclusions | 54 |
| 3.6 | Appendix - Model Validation (SST and Chlorophyll-a) | 55 |
| 3.7 | acknowledgments | 58 |
| 4 | Considerações Finais | 59 |
| | Bibliografia | 61 |

Capítulo

1

Introdução

1.1 Ciclo do Carbono no ambiente marinho

O reservatório de carbono presente nos oceanos contém aproximadamente 60 vezes mais carbono do que na atmosfera. As estimativas pré-industriais dos reservatórios de carbono são de 1000 Pg C nos oceanos superficiais e de 37000 Pg C nos oceanos profundos, enquanto a atmosfera possui aproximadamente 600 Pg C. Os oceanos controlam a concentração de carbono atmosférico por meio de fluxos de CO₂ na interface oceano-atmosfera, que por sua vez impactam o sistema climático devido à propriedades de efeito estufa deste gás. Logo, o ciclo do carbono no ambiente marinho apresenta grande importância para o entendimento do papel dos oceanos na regulação climática natural e também é influenciado por ações antrópicas ([Sarmiento and Gruber, 2006](#)).

O dióxido de carbono (CO₂) ao reagir com a água do mar se dissolve formando dióxido de carbono dissolvido (CO₂^{*}), íons bicarbonato (HCO₃⁻) e carbonato (CO₃²⁻), no chamado sistema ácido carbônico - carbonato - bicarbonato. Todas essas espécies de carbono são chamadas coletivamente de carbono inorgânico dissolvido (DIC),

$$DIC = [CO_2^*] + [HCO_3^-] + [CO_3^{2-}], \quad (1.1)$$

enquanto as trocas entre oceano e atmosfera ocorrem na forma de CO₂, na água do mar 90% do DIC está na forma de íons bicarbonato, 9% está na forma de íons carbonato e apenas o restante 1% na forma de CO₂ dissolvido ([Williams and Follows, 2011](#)).

O transporte vertical de carbono ocorre através de dois processos, um biológico (bomba biológica), a partir da fixação de carbono inorgânico dissolvido em carbono orgânico que posteriormente é transferido na cadeia trófica e pode ser transportado para o fundo como fluxos de agregados de carbono orgânico particulado. O outro processo é físico (bomba de solubilidade) que transporta carbono inorgânico dissolvido, entre oceano e atmosfera e entre diferentes massas de água. Esses dois processos são interconectados no ciclo do carbono através da fixação fotosintética e da remineralização da matéria orgânica ([Hofmann et al., 2011](#)).

O transporte vertical de carbono orgânico particulado inicia-se pela formação de agregados orgânicos, provenientes da produção primária e secundária. Esses agregados são exportados para baixo da zona eufótica por processos de mistura, advecção, difusão, afundamento passivo e transporte ativo (excreção do zooplâncton). O fluxo desta matéria orgânica tende a decrescer com o aumento da profundidade devido ao consumo heterotrófico ([Burd et al., 2010](#)).

Para que ocorra a exportação de ambas as espécies de carbono para o oceano profundo, é necessário que ocorra uma sequência de processos físicos, inicialmente para aumentar a produção primária em superfície ou aumentar o fluxo de carbono inorgânico dissolvido para o oceano, secundariamente para favorecer o afundamento e aprisionamento desses elementos abaixo da camada de mistura ([Fennel, 2010](#)).

As concentrações de carbono inorgânico dissolvido (bomba de solubilidade) aumentam com a profundidade, primariamente pelo aumento da solubilidade em águas mais frias e em maiores pressões e pelo transporte físico de massas de águas frias ricas em carbono da superfície para o fundo. A transferência de carbono orgânico pela atividade biológica também leva a um aumento na concentração de carbono inorgânico dissolvido em águas profundas, através da decomposição (oxidação) da matéria orgânica durante a sedimentação, podendo ser a fonte responsável por até 10% de carbono inorgânico dissolvido em águas profundas ([Williams and Follows, 2011](#)).

1.1.1 Fluxos líquidos de CO₂ na interface oceano-atmosfera

A troca de dióxido de carbono entre atmosfera e oceano, ocorre na camada de mistura dos oceanos (aproximadamente 100m), a camada de mistura e a atmosfera possuem aproximadamente a mesma quantidade de carbono. Na última década estima-se que os oceanos absorveram em média 2.6 ± 0.5 Pg de carbono atmosférico por ano ([Le Quéré et al., 2014](#)), o conhecimento da variabilidade dos fluxos de carbono na interface oceano-atmosfera apresenta importância para previsões em relação às mudanças climáticas. Sem o entendimento do ciclo natural do carbono e de seus fluxos entre os reservatórios, ficamos limitados para verificar a presença de CO₂ proveniente de combustíveis fósseis nos oceanos e também para estimar os futuros níveis atmosféricos de CO₂ realisticamente ([Sabine et al., 2013](#)).

Os fluxos líquidos de CO₂ nesta interface são dependentes da solubilidade do CO₂, da intensidade dos ventos e da diferença entre a pressão parcial do CO₂ na superfície do oceano ($p\text{CO}_2\text{mar}$) e na atmosfera ($p\text{CO}_2\text{ar}$). Como o coeficiente de transferência do gás pelo vento e o $p\text{CO}_2$ atmosférico apresentam baixa variabilidade, o $p\text{CO}_2$ da superfície do oceano será o principal parâmetro para caracterizar os fluxos entre oceano e atmosfera ([Sarmiento and Gruber, 2006](#); [Takahashi et al., 2002](#)). Se o $p\text{CO}_2$ da superfície do oceano for maior que o $p\text{CO}_2$ atmosférico, o oceano irá se comportar como uma fonte de CO₂ para atmosfera, caso o $p\text{CO}_2$ da superfície do oceano for menor que o $p\text{CO}_2$ atmosférico, o oceano irá se comportar como um sumidouro.

Nos oceanos, o $p\text{CO}_2$ é dependente da concentração de *DIC*, da salinidade, da temperatura e da alcalinidade total (*ALK*) ou pH, essas são conhecidas como as variáveis de estado do $p\text{CO}_2$. A alcalinidade total é definida como:

$$\text{ALK} = [\text{HCO}_3^-] + 2[\text{CO}_3^{2-}] + [\text{OH}^-] - [\text{H}^+] + [\text{B(OH)}_4^-] + \dots, \quad (1.2)$$

é uma medida do excesso de bases sobre os ácidos, assim no final da equação são somados os íons e cátions de elementos menores ([Williams and Follows, 2011](#)).

Salinidade e temperatura são diretamente proporcionais ao $p\text{CO}_2$, no entanto há uma maior sensibilidade da temperatura relacionada à solubilidade do CO₂. Ou seja, com um resfriamento

da água há um aumento na solubilidade, levando a uma diminuição no $p\text{CO}_2$. Inversamente, com um aquecimento há uma diminuição da solubilidade, levando a um aumento no $p\text{CO}_2$. O DIC também apresenta um comportamento diretamente proporcional ao $p\text{CO}_2$, no entanto inversamente proporcional à temperatura, ou seja águas mais quentes possuem menor concentração de DIC do que águas frias, logo com efeitos contrastantes às mudanças de solubilidade. Já a ALK é a única variável de estado com comportamento inversamente proporcional ao $p\text{CO}_2$ ([Sarmiento and Gruber, 2006](#)).

As variáveis de estado são, por sua vez, afetadas por processos físicos e biológicos. Enquanto a salinidade e temperatura dependem apenas de processos físicos, o DIC e a ALK são afetados tanto por processos físicos como biológicos. Assim, os fluxos líquidos de CO_2 serão dependentes da interação de vários fatores como: solubilidade, fixação biológica de DIC , produção e dissolução de CaCO_3 , ressurgência e mistura de águas com elevadas concentrações de nutrientes e DIC , velocidade do vento, e fluxos de água doce que irão diluir as concentrações de DIC e ALK ([Doney et al., 2009](#)).

No geral, os oceanos tropicais ($14^{\circ}\text{N} - 14^{\circ}\text{S}$) possuem elevados valores de $p\text{CO}_2$, caracterizando esses oceanos como fontes de CO_2 para a atmosfera. Já nos oceanos temperados ($14^{\circ} - 50^{\circ}$), há uma grande variabilidade sazonal, com o $p\text{CO}_2$ geralmente abaixo do nível atmosférico no inverno caracterizando esses oceanos como sumidouros de carbono atmosférico, e o inverso ocorrendo no verão, com elevados valores de $p\text{CO}_2$ e um comportamento de fonte para a atmosfera([Takahashi et al., 2002](#)).

1.1.2 Papel das plataformas continentais

As plataformas continentais são regiões rasas e estreitas, apresentando aproximadamente 200 metros de profundidade e 200 quilômetros de extensão, possuindo uma declividade suave (1:100). São regiões especiais do oceano global devido aos fluxos de materiais terrígenos e às elevadas produções primária e secundária ([Christensen, 1994](#)). Esses ambientes ocupam cerca de 7 a 10% do oceano global ([Laruelle et al., 2013](#)), mas estima-se que a contribuição para a produção primária global seja de 19-28% ([Longhurst et al., 1995](#)).

Para a compreensão do ciclo do carbono na plataforma continental devem ser considerados os aportes de água doce, sedimento, nutrientes e carbono de origem terrígena, o fluxo dos elementos nas interfaces sedimento-água e atmosfera-oceano, a ciclagem dos elementos no interior da coluna de água, e as trocas entre plataforma continental e o oceano profundo ([Hofmann et al., 2011](#)).

As plataformas continentais constituem um importante componente do sistema biogeoquímico do planeta, apesar disso a contribuição das plataformas para o ciclo do carbono oceânico ainda permanece pobramente estimada e compreendida. Como essas regiões rasas do oceano recebem maior impacto da atividade humana, um maior esforço têm sido feito para o entendimento dos processos que afetam os fluxos de carbono e nutrientes nessas regiões ([Liu et al., 2010](#)). No entanto, ainda há incertezas em relação ao comportamento médio global das plataformas continentais, isto é, se atuam como fonte ou sumidouro de CO₂. Estas incertezas devem-se ao fato de que os principais modelos globais excluem os mares costeiros de seus domínios ([Takahashi et al., 2009](#)).

A primeira estimativa da contribuição global das plataformas foi de uma absorção de 1 Pg de carbono por ano ([Tsunogai et al., 1999](#)), extrapolando um estudo realizado na plataforma ao leste da China, caracterizando a área como um sumidouro de CO₂ dominado pela bomba de solubilidade. Estimativas mais recentes variam entre 0,2 e 0,5 Pg C por ano ([Chen et al., 2013; Laruelle et al., 2013; Yool and Fasham, 2001](#)), apesar da diminuição nas estimativas de absorção de carbono nas plataformas, este ainda é um valor extremamente importante, representando em torno de 20 - 30 % do total de carbono absorvido pelo oceano global.

No geral, as plataformas continentais seguem o comportamento encontrado no oceano aberto, com plataformas em altas e médias latitudes subsaturadas em relação ao CO₂ atmosférico, atuando como sumidouro, e plataformas em baixas latitudes atuando, na média, como fracas fontes de CO₂ para a atmosfera ([Chen et al., 2013; Laruelle et al., 2013](#)). No entanto as plataformas apresentam maior variabilidade espacial e temporal devido à interação entre resfriamento/aquecimento, elevada produção biológica que consome DIC, ressurgências e mistura da coluna de água aumentando a concentração de DIC na superfície e o suprimento fluvial/terrígeno de carbono orgânico e inorgânico ([Gruber, 2015](#)).

Devido a elevada variabilidade do $p\text{CO}_2$, e consequentemente de fluxos líquidos de CO_2 nas plataformas continentais, são necessários estudos mais detalhados tanto espacial como temporalmente para uma caracterização precisa desses ambientes. No mar do Norte por exemplo, foi identificada uma compartmentalização durante o verão, com a porção mais ao Norte absorvendo CO_2 atmosférico e ao Sul ocorrendo liberação de CO_2 para a atmosfera (Thomas et al., 2004; Bozec et al., 2005). As diferenças entre plataformas internas e externas também são substanciais, geralmente as plataformas internas atuam como fonte de CO_2 enquanto as externas atuam como sumidouro (Cai, 2003). Este padrão pode ser explicado pela diminuição do aporte de carbono terrígeno, aumento da produção primária devido a diminuição da turbidez da água nas plataformas média e externa, e aumento do aporte de nutrientes através de ressurgência e mistura na quebra de plataforma (Walsh, 1991).

1.2 Área de Estudo e antecedentes

A área de estudo no oceano Atlântico Sudoeste está situada entre 15°S e 55°S e entre 70°W e 35°W . Esta região é caracterizada pela confluência das correntes superficiais do Brazil e das Malvinas, dividindo os giros subtropicais e subantárticos em torno de $35\text{-}40^{\circ}\text{S}$ (Frente Subtropical), e caracterizando essa região como uma das mais energéticas do oceano global (Piola and Matano, 2001) (Fig. 1.1).

A região subtropical é caracterizada por uma coluna de água bem estratificada durante todo o ano, com baixas concentrações de nutrientes na superfície, sendo caracterizada como um bioma subtropical permanentemente estratificado. Já a região subantártica apresenta uma profunda camada de mistura durante o inverno possibilitando a fertilização das águas superficiais, e durante o verão/primavera a coluna de água estratificada possibilita elevadas taxas de produção primária, sendo caracterizada como um bioma subtropical sazonalmente estratificado (Sarmiento et al., 2004).

A plataforma da Patagônia ao Sul do domínio é uma das maiores plataformas continentais do mundo, alcançando até 800 km da linha de costa. Ao Norte, as plataformas do Sul e Sudeste do Brasil são mais estreitas, alcançando em torno de 100-200 km da linha de costa. Ao longo

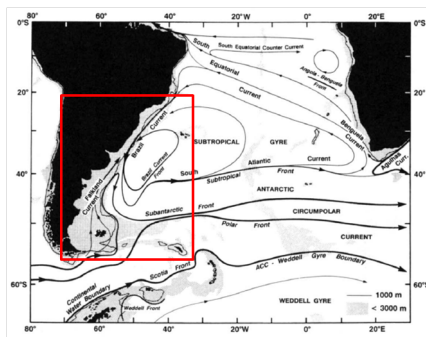


Figura 1.1: Representação da área de estudo (retângulo vermelho) e das correntes superficiais do giro subtropical do oceano Atlântico Sul, adaptado de [Peterson and Stramma \(1991\)](#).

das plataformas continentais a circulação superficial é influenciada e direcionada pelas correntes de contorno. No entanto, a circulação é modificada pela topografia, ventos, amplitudes de maré, aportes fluviais e ressurgências costeiras ([Castro and Miranda, 1998](#); [Piola et al., 2000](#); [Matano et al., 2010](#)). As ressurgências costeiras ocorrem em locais específicos das plataformas Sul e Sudeste do Brasil, como em Cabo Frio e no Cabo de Santa Marta, devido principalmente aos padrões de ventos e à mudança da direção da linha de costa ([Ciotti et al., 2014](#)). Devido as diversas feições e forçantes encontradas nas plataformas continentais do domínio em estudo, é importante salientar que estamos lidando com várias províncias biogeoquímicas ou ecológicas ([Gonzalez-Silveira et al., 2004](#)).

Nas plataformas continentais brasileiras existem poucos estudos sobre fluxos líquidos de CO₂. A Plataforma Sudeste foi caracterizada como fonte de CO₂ para a atmosfera durante todas as estações do ano e foi sugerido que o efeito da temperatura, os processos biológicos e os processos físicos de mistura são os principais contribuidores para as variações destes fluxos na plataforma continental ([Ito et al., 2005](#)). Já na Plataforma Patagônica, a plataforma interna foi identificada como fonte de carbono para atmosfera, enquanto as plataformas média e externa foram identificadas como sumidouros, sugerindo que os processos biológicos devem ser o principal regulador da variabilidade do pCO₂ na região ([Bianchi et al., 2009](#); [Schloss et al., 2007](#)).

1.3 Objetivos

Objetivo geral:

Caracterizar o comportamento *offshore* e nas plataformas continentais no oceano Atlântico Sudoeste em relação à variabilidade dos fluxos de carbono na interface oceano-atmosfera.

Objetivos específicos:

- Validação do modelo biogeoquímico NPZD (Nitrogênio, Fitoplâncton, Zooplâncton e Detritos) utilizado;
- Analisar e avaliar a variabilidade espaço-temporal do $p\text{CO}_2$ superficial modelado;
- Verificar quais são as principais variáveis controladoras das anomalias de $p\text{CO}_2$ superficial;
- Identificar quais os processos que mais impactam o $p\text{CO}_2$;
- Quantificar os fluxos líquidos de CO_2 entre oceano e atmosfera na região de estudo.

1.4 Motivação

A investigação e o esforço observacional a respeito dos fluxos de carbono na interface oceano-atmosfera têm aumentado significativamente nas últimas décadas, principalmente à luz das mudanças climáticas e do impacto da atividade humana. O banco de dados Surface Ocean CO_2 Atlas (SOCAT) conta hoje com a sua versão atualizada com mais de 10 milhões de observações in-situ de $f\text{CO}_2$ (fugacidade do CO_2 , levando em consideração o comportamento não ideal deste gás) entre os anos 1968 e 2011 ([Bakker et al., 2013](#)).

Apesar disso, o oceano Atlântico Sudoeste é uma região pouco investigada, com poucas observações e muitas lacunas, especialmente nas plataformas continentais. Logo, este trabalho representa um passo inicial para a avaliação dos fluxos líquidos de CO_2 e do comportamento do $p\text{CO}_2$ superficial nesta região como um todo, através de modelagem numérica biogeoquímica.

A utilização de modelos numéricos é justificada pela possibilidade de investigar processos que são de difícil mensuração, como por exemplo o efeito da produção biológica na variabilidade do $p\text{CO}_2$. Além disso, a partir deste trabalho inicial de modelagem biogeoquímica, o modelo poderá ser refinado com advento de novas observações e diferentes processos poderão ser investigados utilizando este trabalho como linha de base.

Capítulo

2

Métodos

2.1 Modelo

Foram utilizados modelos numéricos, para simular os mecanismos dinâmicos que dirigem a circulação oceânica, a produtividade e a ciclagem do carbono na coluna de água. Para isso, foram utilizados módulos biogeoquímicos baseados na relação entre nutrientes, fitoplâncton, zooplânctôn e detritos (NPZD), acoplados ao sistema de modelagem hidrodinâmica do *Regional Ocean Modeling System* (ROMS) versão UCLA - Universidade da Califórnia.

O modelo hidrodinâmico ROMS é um modelo de circulação oceânica de nova geração, tendo sido desenvolvido especialmente para simulações de sistemas oceânicos regionais. Este modelo resolve as equações primitivas do movimento, baseadas na aproximação de Boussinesq e no balanço hidrostático, de superfície livre e com coordenadas verticais que seguem a topografia. Na horizontal, utiliza coordenadas curvilineares em uma grade do tipo Arakawa–C ([Shchepetkin and McWilliams, 2005, 2009](#)).

O modelo ROMS tem sido amplamente utilizado em estudos de circulação de plataformas continentais acoplado com aplicações físico-biológicas. Este modelo reproduz com acurácia a evolução de traçadores, sendo uma característica atrativa para a modelagem biogeoquímica, pois facilita a interação entre os traçadores e possibilita cálculos de balanço de nutrientes e carbono ([Hofmann et al., 2011](#)).

O módulo biogeoquímico, ou ecológico, que foi utilizado é um modelo do tipo NPZD baseado

no elemento nitrogênio. Este modelo consiste de um sistema de 7 equações diferenciais que governam a distribuição espacial e temporal de 7 escalares não-conservativos. Esses escalares são: Nitrato, Amônio, Fitoplâncton, Zooplâncton, Detritos pequenos, Detritos Grandes, e uma razão dinâmica entre clorofila e carbono do fitoplâncton. Além desses escalares, este modelo também possui uma componente de carbono, com a adição de DIC , $CaCO_3$ e alcalinidade ([Gruber et al., 2006](#); [Lachkar and Gruber, 2013](#)).

A equação de conservação para qualquer um dos 7 escalares é dada por:

$$\frac{\partial B}{\partial t} = \Delta \cdot K \Delta B - u \cdot \Delta_h B - (w + w^{sink}) \frac{\partial B}{\partial z} + J(B) \quad (2.1)$$

onde K é o tensor de difusividade cinemática turbulenta, u e w são as velocidades horizontais e verticais, e w^{sink} é a taxa de afundamento dos componentes biogeoquímicos. O termo $J(B)$ representa os termos fontes menos os termos sumidouros de cada um dos 7 escalares, representado no diagrama da Fig.2.1 ([Gruber et al., 2006](#)). Assim, o fitoplâncton por exemplo, possui um termo fonte representando o crescimento dependente da luz e da concentração de nitrato e/ou amônio, e 3 termos de perda representando mortalidade, pastagem pelo zooplâncton e coagulação em detritos.

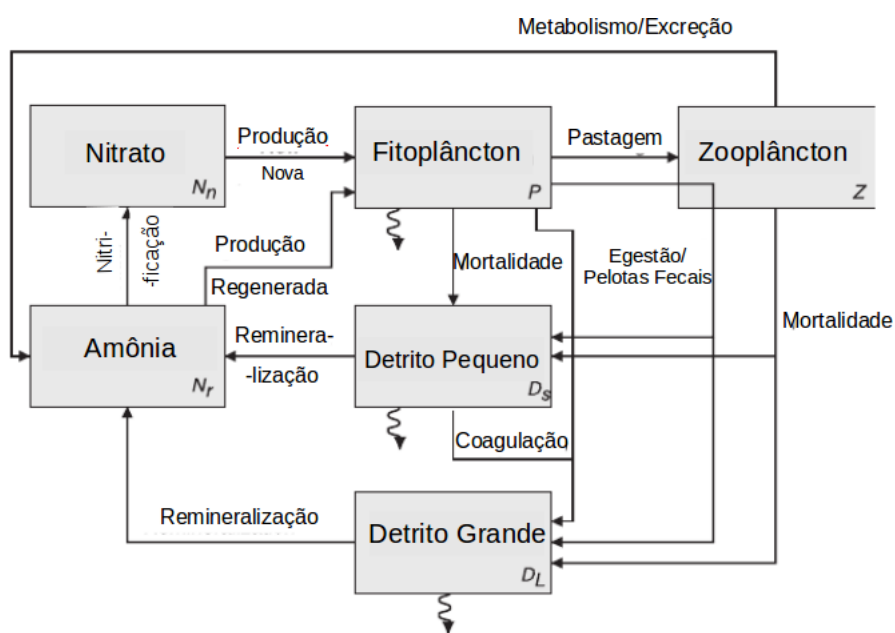


Figura 2.1: Diagrama do modelo NPZD representando as fontes e os sumidouros para cada módulo biogeoquímico, adaptado de [Gruber et al. \(2006\)](#).

2.2 Análises

2.2.1 Cálculo $p\text{CO}_2$

O $p\text{CO}_2$ superficial foi calculado utilizando as variáveis DIC , ALK , temperatura e salinidade com o programa CO2SYS ([Van Heuven et al., 2009](#)). Temperatura e salinidade são utilizadas para o cálculo das constantes de dissociação k_0 , k_1 e k_2 , que aqui foram utilizadas as equações de [Millero \(1995\)](#). O pH é calculado iterativamente através de DIC e ALK , assim chega-se às concentrações de H^+ .

Primeiramente é calculado a fugacidade ($f\text{CO}_2$), que leva em conta o comportamento não ideal do CO_2 a partir da seguinte equação:

$$f\text{CO}_2 = \frac{DIC}{K_0} \cdot \frac{[H^+]^2}{[H^+]^2 + [H^+].K_1 + K_1.K_2} \quad (2.2)$$

Para calcular o fator de fugacidade do CO_2 (FugFac) foi utilizada a seguinte relação:

$$\text{FugFac} = e^{((B+2\Delta).p1atm/RT)} \quad (2.3)$$

onde B e Δ são funções dependentes da temperatura, $P1\text{atm}$ é a pressão no nível do mar, R é a constante universal dos gases e T é a temperatura [Körtzinger \(1999\)](#). Finalmente, o $p\text{CO}_2$ é calculado como:

$$p\text{CO}_2 = f\text{CO}_2 / \text{FugFac} \quad (2.4)$$

2.2.2 Estatísticas para avaliação do modelo

Para comparar o $p\text{CO}_2$ modelado com a base de dados do SOCAT, foram utilizados os seguintes indicadores estatísticos: Eficiência do Modelo (ME)([Nash and Sutcliffe, 1970](#)), função custo (CF)([Ospar et al., 1998](#)) e percentagem de erro (PB)([Allen et al., 2007](#)).

$$ME = 1 - \frac{\sum(O - M)^2}{\sum(O - \bar{O})^2} \quad (2.5)$$

$$CF = \frac{\Sigma |(M - O)|}{n\sigma} \quad (2.6)$$

$$PB = \left| \frac{\Sigma(O - M)}{\Sigma O} \cdot 100 \right| \quad (2.7)$$

onde O são observações, M são resultados do modelo, \bar{O} é a média espaço-temporal das observações na área analisada, n é o número de observações disponíveis e σ é o desvio padrão das observações. Essas estatísticas proporcionam informações adicionais sobre a performance do modelo. Utilizando ME o modelo pode ser caracterizado como excelente ($ME > 0.65$), muito bom ($0.5 < ME < 0.65$), bom ($0.2 < ME < 0.5$) ou ruim ($ME < 0.2$). Já o indicador CF pode caracterizar o modelo como excelente ($CF < 1$), bom ($1 < CF < 2$), regular ($2 < CF < 3$) ou ruim ($CF > 3$). Por fim, o indicador PB pode caracterizar o modelo como excelente ($PB < 10$), muito bom ($10 < PB < 20$), bom ($20 < PB < 40$) ou ruim ($PB > 40$).

2.2.3 Cálculo dos Controladores

Para calcular o impacto de cada uma das variáveis de estado, o pCO_2 foi decomposto em relação à temperatura, salinidade, DIC and ALK , segundo Lovenduski et al. (2007); Doney et al. (2009); Turi et al. (2014); Signorini et al. (2013),

$$\Delta pCO_2 = \frac{\partial pCO_2}{\partial DIC} \Delta DIC^s + \frac{\partial pCO_2}{\partial ALK} \Delta ALK^s + \frac{\partial pCO_2}{\partial T} \Delta T + \frac{\partial pCO_2}{\partial FW} \Delta FW \quad (2.8)$$

,

onde os Δs são as anomalias, espaciais ou temporais. ALK^s e DIC^s são as concentrações normalizadas pela salinidade média superficial do domínio, e FW é o efeito da salinidade excluindo mudanças relativas a diluição de DIC e ALK . As derivadas parciais foram calculadas segundo Doney et al. (2009) utilizando a seguinte equação:

$$\frac{\partial pCO_2}{\partial X_i} = \frac{pCO_2(\bar{X}_i + X'_i, \bar{X}_j) - pCO_2(\bar{X}_i, \bar{X}_j)}{X'_i} \quad (2.9)$$

Onde \bar{X}_i é a média da variável e X'_i é a perturbação. Assim a influência de cada controlador

foi calculada, mantendo 3 variáveis fixas na média e adicionando uma perturbação para a variável de interesse.

2.2.4 Estimativa dos processos reguladores

Para a estimativa dos principais processos reguladores do $p\text{CO}_2$ foram feitos 3 experimentos adicionais, excluindo aditivamente os processos de fluxo de CO_2 na interface oceano-atmosfera, produção biológica e solubilidade do CO_2 . Para tal, no primeiro experimento (E1) o fluxo de CO_2 na interface foi fixado em 0. No segundo experimento (E2), adicionalmente à alteração em E1, a radiação fotossinteticamente ativa (PAR) foi fixada em 0, evitando a produção primária. E no terceiro experimento (E3), adicionalmente às mudanças em E1 e E2, a solubilidade do CO_2 foi fixada a um valor constante, calculado utilizando as médias superficiais de temperatura e salinidade do domínio ([Turi et al., 2014](#)). A tabela 2.1 resume os experimento e como foi calculado a contribuição de cada processo para o $p\text{CO}_2$.

Assim, assumindo que os impactos desses processos no $p\text{CO}_2$ são linearmente aditivos, o $p\text{CO}_2$ modelado foi decomposto em 4 componentes:

$$p\text{CO}_2^{\text{controle}} = p\text{CO}_2^{\text{fluxo-oceano-atm}} + p\text{CO}_2^{\text{biologia}} + p\text{CO}_2^{\text{solubilidade}} + p\text{CO}_2^{\text{Transporte}} \quad (2.10)$$

Tabela 2.1: Detalhe dos experimentos para estimativa do efeito dos processos na variabilidade do $p\text{CO}_2$ ([Turi et al., 2014](#))

| Experimento | Alterações |
|---------------|--|
| Controle | Sem alterações |
| E1 | Sem fluxos oceano-atmosfera |
| E2 | Sem fluxos oceano-atmosfera, sem biologia |
| E3 | Sem fluxos oceano-atmosfera, sem biologia e com solubilidade cte |
| Cálculo | Processos |
| Controle - E1 | Contribuição do Fluxo oceano-atmosfera |
| E1 - E2 | Contribuição da produção biológica |
| E2 - E3 | Contribuição da solubilidade do $p\text{CO}_2$ |
| E3 | Contribuição do transporte físico |

Capítulo

3

Manuscrito

Air-sea CO_2 fluxes and the controls on ocean surface pCO_2
variability in coastal and open-ocean southwestern Atlantic
Ocean: A modeling study

Ricardo Arruda¹, Paulo H. R. Calil¹, Alejandro A. Bianchi^{2,3}, Scott C. Doney⁴, Nicolas Gruber⁵, Ivan Lima⁴, and Giuliana Turi^{5,6}

¹Laboratório de Dinâmica e Modelagem Oceânica (DinaMO), Instituto de Oceanografia,
Universidade Federal do Rio Grande, Rio Grande, RS, Brazil.

²Departamento de Ciencias de la Atmósfera y los Océanos, Universidad de Buenos Aires,
Buenos Aires, Argentina.

³Departamento Oceanografía, Servicio de Hidrografía Naval, Av. Montes de OCA2124-
Buenos Aires, Argentina

⁴Department of Marine Chemistry and Geochemistry, Woods Hole Oceanographic
Institution, Woods Hole, MA, USA.

⁵Institute of Biogeochemistry and Pollutant Dynamics, ETH, Zurich, Switzerland.

⁶Now at: CIRES, University of Colorado at Boulder, and NOAA/ESRL, Boulder, CO,
USA.

Abstract

We use an eddy-resolving, regional ocean biogeochemical model to investigate the main variables and processes responsible for the climatological spatio-temporal variability of $p\text{CO}_2$ and the air-sea CO_2 fluxes in the southwestern Atlantic Ocean. Overall, the region acts as sink of atmospheric CO_2 south of 30°S , and is close to equilibrium with the atmospheric CO_2 to the north. On the shelves, the ocean acts as a weak source of CO_2 , except for the mid/outer shelves of Patagonia, which act as sinks. In contrast, the inner shelves and the low latitude open ocean of the southwestern Atlantic represent source regions. Observed nearshore-to-offshore and meridional $p\text{CO}_2$ gradients are well represented by our simulation. A sensitivity analysis shows the importance of the counteracting effects of temperature and dissolved inorganic carbon (DIC) in controlling the seasonal variability of $p\text{CO}_2$. Biological production and solubility are the main processes regulating $p\text{CO}_2$, with biological production being particularly important on the shelf regions. The role of mixing/stratification in modulating DIC , and therefore surface $p\text{CO}_2$ is shown in a vertical profile at the location of the Ocean Observatories Initiative (OOI) site in the Argentine Basin ($42^\circ\text{S}, 42^\circ\text{W}$).

3.1 Introduction

Shelf regions are amongst the most biogeochemically dynamical zones of the marine biosphere (Walsh, 1991; Bauer et al., 2013). Even though they comprise only 7 – 10% of the global ocean area (Laruelle et al., 2013), continental shelves could contribute to approximately 10 – 15% of the ocean primary production and 40% of the ocean’s carbon sequestration (Muller-Karger et al., 2005). Global discussions about the role of continental margins as a sink of atmospheric CO₂ gained momentum after Tsunogai et al. (1999), who suggested that these shelf regions take up as much as 1 PgC/year of atmospheric CO₂. Recent estimates range from 0.2 PgC/year (Laruelle et al., 2013) to 0.589 PgC/year (Yool and Fasham, 2001), somewhat more modest than initially thought (Gruber, 2015), but still relevant to the global ocean absorption estimated around 2.3 PgC/year (Ciais et al., 2014).

Continental shelves tend to act as a sink of carbon at high and medium latitudes (30° – 90°), and as a weak source at low latitudes (0° – 30°) (Chen et al., 2013; Hofmann et al., 2011; Bauer et al., 2013; Laruelle et al., 2014), i.e., they tend to follow similar meridional trends as the open ocean CO₂ fluxes (Landschützer et al., 2014; Takahashi et al., 2009).

However, continental shelves present a higher spatio-temporal variability of air-sea CO₂ fluxes than the adjacent open ocean, with the inner shelf and near coastal regions generally acting as a source of CO₂ to the atmosphere, while the mid/outer shelf and the continental slope generally acting as sink (Cai, 2003). This pattern can be explained by the increased primary production in the inner shelf and decreased terrestrial supply towards the outer shelf (Walsh, 1991). Seasonality of the upper ocean (e.g. mixing and stratification) may also be important to the air-sea exchange of carbon. For example, the United States southeast continental shelf acts as a sink of CO₂ in the winter and as a source in the summer (Wang et al., 2005).

In the southwestern Atlantic Ocean, the shelf region presents distinct features. To the south, the Patagonian shelf is one of the world’s largest shelves with an area close to 10⁶ km², broadening to more than 800 km from the coastline (Bianchi et al., 2009). To the north, the Brazilian shelf narrows to around 100-200 km from the coastline. In the offshore This region is characterized as one of the most energetic regions of the world’s ocean with the confluence of the warm southward-

flowing Brazil Current (BC) and the cold Malvinas Current (MC) flowing northward ([Piola and Matano, 2001](#)). The extension of the confluence roughly divides the subtropical and subantarctic oceanic gyres in the South Atlantic and maybe a hotspot for shelf-open ocean exchange ([Guerrero et al., 2014](#)).

This area is thought to absorb between 0.3-0.6 PgC/year south of $30^{\circ}S$, while acting as a source to the atmosphere north of $30^{\circ}S$ ([Takahashi et al., 2002](#)). Aside from global estimates, only a few local studies were conducted on the continental shelves in this region. The Patagonian shelf was characterized as a source of CO₂ to the atmosphere on the inner shelf, and as a sink in the mid-outer shelf ([Bianchi et al., 2009](#)). The southeast Brazilian shelf and continental slope were characterized as sources of CO₂ to the atmosphere during all seasons ([Ito et al., 2005](#)). Such regions are often neglected, or poorly resolved, on relatively coarse global modelling assessments, although they may contribute up to 0.2 PgC/year of global ocean CO₂ uptake ([Laruelle et al., 2014](#)).

Regional marine biogeochemical models have been used to assess the ocean carbonate system and CO₂ fluxes, including the continental margins. For example, along the US east coast, the seasonality of $p\text{CO}_2$ was found to be controlled mainly by changes in the solubility of CO₂ and biological processes ([Fennel and Wilkin, 2009](#)). Along the California coast, biological production, solubility and physical transport (e.g. circulation) were found to be the most influential processes on $p\text{CO}_2$ variability, both spatial and temporal ([Turi et al., 2014](#)).

In this study we use a regional marine biogeochemical model coupled to a hydrodynamic model to investigate the drivers and processes regulating the variability of ocean surface $p\text{CO}_2$ in the southwestern Atlantic Ocean. Our model domain includes the region of the soon to be deployed Ocean Observatories Initiative (OOI) Argentine global node at 42°S , 42°W ([oceanobservatories.org](#)).

We compare modeled surface $p\text{CO}_2$ distribution with observations and use the results to investigate the relative importance of the drivers (*DIC*, temperature, alkalinity and salinity) and processes (biological production, air-sea CO₂ flux, CO₂ solubility and physical transport) in controlling surface $p\text{CO}_2$ distribution and variability on the continental shelf and open ocean

in the southwestern Atlantic Ocean.

3.2 Materials and Methods

3.2.1 Model

The physical model used in this study is the Regional Ocean Modeling System (ROMS) ([Shchepetkin and McWilliams, 2005](#)). Our model domain in the southwestern Atlantic Ocean spans from subtropical to subantarctic oceanic regions ($15^{\circ}S$ to $55^{\circ}S$) and from the continental shelves to the open ocean ($70^{\circ}W$ to $35^{\circ}W$). The horizontal grid resolution is 9 km, with 30 vertical levels with increasing resolution towards the surface.

The biogeochemical model is an NPZD type, including the following state variables: phytoplankton, zooplankton, nitrate, ammonium, small and large detritus, and a dynamic chlorophyll to carbon ratio for the phytoplankton ([Gruber et al., 2006](#)). A carbon component is also coupled to the model, with the addition of calcium carbonate, *DIC* and alkalinity to the system of state variables ([Gruber et al., 2011; Hauri et al., 2013; Turi et al., 2014](#)). Parameters utilised in the biogeochemical model are listed in Table 3.1. These parameters tend to favour large phytoplankton types in relatively eutrophic regions ([Gruber et al., 2006](#)). Since our domain encompasses several ecological provinces ([Gonzalez-Silveira et al., 2004](#)), we may not represent all regions equally well with only one phytoplankton functional type.

The initial and boundary conditions used for the physical variables were obtained from a climatology of the Simple Ocean Data Assimilation (SODA) ([Carton and Giese, 2008](#)), and for the biogeochemical variables from a Community Earth System Model (CESM) climatological model product. The model is forced with climatological winds from QuikSCAT and heat and freshwater surface fluxes from the Comprehensive Ocean-Atmosphere Data Set (COADS) ([Da Silva et al., 1994](#)). We used a fixed atmospheric $p\text{CO}_2$ of $370 \mu\text{atm}$ without CO_2 incrementation throughout the years. Starting from rest we ran the model for 8 years and used a climatology from years 5 through 8 for our analyses.

Since we are mostly concerned with climatological analysis, we chose not to represent pro-

cesses such as river run-off and tides, which can be locally important. Nevertheless, the low salinity waters from the La Plata river are indirectly included as the model nudges to climatological salinity values in the region. The lack of tides may adversely affect our model results in the inner shelf of Patagonia, where tidal amplitudes reach up to 12 meters at some points (Kantha, 1995; Saraceno et al., 2010) and tidal fronts are known to impact oceanic $p\text{CO}_2$ (Bianchi et al., 2005). Despite these local shortcomings our model results should not be significantly affected in the overall climatological estimates of the drivers and processes controlling $p\text{CO}_2$ in our domain. These processes will be implemented in future studies.

Table 3.1: Parameters of the biogeochemical model as in Gruber et al. (2006)

| Parameter | Value | units |
|---|--------|---|
| Seawater light attenuation | 0.04 | m^{-1} |
| Chl-a light attenuation | 0.024 | $\text{m}^{-1}(\text{mgChlam}^{-3})^{-1}$ |
| Carbon to Nitrogen ratio | 6.625 | |
| Precipitation of CaCO_3 | 0.07 | |
| Dissolution of CaCO_3 | 0.0057 | day^{-1} |
| Phytoplankton Half-sat. for nitrate uptake | 0.75 | mmolm^{-3} |
| Phytoplankton Half-sat. for ammonium uptake | 0.50 | mmolm^{-3} |
| Phytoplankton linear mortality rate | 0.024 | day^{-1} |
| max chlorophyll/carbon ratio | 0.0535 | mgChla/mgC |
| Zoo. Grazing rate | 0.6 | day^{-1} |
| Zoo. Assimilation efficiency | 0.75 | |
| Grazing half-sat. for Phytoplankton | 1.0 | mmolNm^3 |
| Zoo. Mortality rate | 0.1 | $\text{day}^{-1}(\text{mmolm}^{-3})^{-1}$ |
| Zoo. Basal metab. rate | 0.1 | day^{-1} |
| Zoo. Mortality alloc. fract. | 0.33 | |
| Zoo. Egestion alloc. fract. | 0.33 | |
| Particle coagulation rate | 0.005 | day^{-1} |
| Nitrification rate | 0.05 | day^{-1} |
| Nitrification inhibition threshold | 0.0095 | Wm^{-2} |
| Nitrification inhibition half dose | 0.036 | Wm^{-2} |
| Remin. ratio of small detritus | 0.03 | day^{-1} |
| Remin. ratio of large detritus | 0.01 | day^{-1} |
| Phytoplankton sinking velocity | 0.5 | mday^{-1} |
| Small detritus sinking velocity | 1.0 | mday^{-1} |
| Large detritus sinking velocity | 10 | mday^{-1} |

3.2.2 Analysis

Ocean surface $p\text{CO}_2$ is the most important variable determining the air-sea CO_2 flux. This is because the variability of ocean $p\text{CO}_2$ is much greater than that of atmospheric $p\text{CO}_2$, and variations in the gas transfer coefficient are usually several times smaller than those of surface ocean

$p\text{CO}_2$ ([Takahashi et al., 2002](#)). Seawater $p\text{CO}_2$ is regulated by the concentration of dissolved inorganic carbon (DIC), total alkalinity (ALK), temperature (T) and salinity (S). While T and S are controlled solely by physical factors, DIC and ALK are affected both by biological production and physical transport. DIC concentration is also affected by air-sea CO_2 fluxes ([Sarmiento and Gruber, 2006](#)).

In our model, surface ocean $p\text{CO}_2$ is calculated through a full model implementation of the seawater inorganic carbon system, as a function of the state variables T , S , DIC , and ALK , with the dissociation constants k_1 and k_2 from [Millero \(1995\)](#). In order to assess the impact of different drivers on $p\text{CO}_2$ variability, we decompose $p\text{CO}_2$ with respect to T , S , DIC and ALK , following the approach of [Lovenduski et al. \(2007\)](#); [Doney et al. \(2009\)](#); [Turi et al. \(2014\)](#); [Signorini et al. \(2013\)](#),

$$\Delta p\text{CO}_2 = \frac{\partial p\text{CO}_2}{\partial \text{DIC}} \Delta \text{DIC}^s + \frac{\partial p\text{CO}_2}{\partial \text{ALK}} \Delta \text{ALK}^s + \frac{\partial p\text{CO}_2}{\partial T} \Delta T + \frac{\partial p\text{CO}_2}{\partial FW} \Delta FW \quad (3.1)$$

,

where the Δ 's are anomalies, either spatial or temporal, DIC^s and ALK^s are the variable concentrations normalized to a domain-averaged surface salinity of 34.66. The freshwater component (FW) is calculated in order to include the effects of precipitation and evaporation on DIC and ALK concentrations.

The partial derivatives were calculated following [Doney et al. \(2009\)](#). $p\text{CO}_2$ was recalculated four times adding a small perturbation to the spatial, or temporal, domain average for each variable (T , S , DIC , ALK) while maintaining the other 3 variables fixed to the domain averaged surface values. The perturbation applied here was 0.1% of the domain mean.

In order to investigate the drivers and processes controlling $p\text{CO}_2$ on the continental margin, we limited our temporal analysis to three regions with depths shallower than 1000 m: the Southeast Brazilian Shelf (SEBS) in the northern part of the domain, the South Brazilian Shelf

(SBS) in the middle of the domain that encompasses the Uruguayan Shelf, and the Patagonian Shelf (PS) to the south of the domain (Fig.3.1a). We also selected two open ocean regions for comparison with the continental shelves: a subtropical (ST) and a subantarctic (SA) region (Fig.3.1b). In each of these regions, we estimated the monthly contribution of each driver to the modeled $p\text{CO}_2$ variability by spatially averaging the variables within each region, and calculating the anomalies by subtracting the annual average from the monthly averages. For the spatial analysis, we used the entire domain and then calculated in each grid cell the spatial anomalies by subtracting the annual mean of that grid cell.

In order to identify the main processes responsible for the variability of surface $p\text{CO}_2$, we used a progressive series of sensitivity experiments as in [Turi et al. \(2014\)](#), focusing on the processes of biological production, CO_2 solubility, air-sea CO_2 fluxes, and physical transport. To quantify these processes, we made three additional model runs, progressively excluding each process. In the first experiment (E1), we set the CO_2 gas exchange flux coefficient between the atmosphere and the ocean to zero, inhibiting gas exchange in the surface layer. In the second experiment (E2), we started from E1 and also turned off the photosynthetically available radiation (PAR), preventing phytoplankton growth. Finally, in experiment E3, the CO_2 solubility was set to a constant value, calculated with domain-averaged surface salinity and temperature of 34.66 and 12.33 °C, respectively, while maintaining the changes of E1 and E2. The control run minus E1 represents the impact of gas exchange between ocean and atmosphere, E1 minus E2 represents the impact of biology, E2 minus E3 represents the impact of variable solubility. The last experiment (E3), in which there is no air-sea flux, no biology and constant solubility represents the impact of physical transport ([Turi et al., 2014](#)).

Given the short model integration times, the vertical gradients in the E3 simulation have not come in to steady-state with the processes. So our physical transport is working on the vertical DIC gradients established by the biological pump. Since the lateral boundary conditions are the same for all experiments, these simulations are therefore only approximations of the impact of each process on $p\text{CO}_2$. Further, this separation assumes a linear additivity of each process, which is clearly a strong simplification given the non-linear nature of the inorganic carbonate system ([Sarmiento and Gruber, 2006](#)). The same spatial and temporal analysis described for the variables (ALK , DIC , T and FW) was also applied for the processes experiments (air-sea CO_2

flux, biology, CO₂ solubility, physical transport).

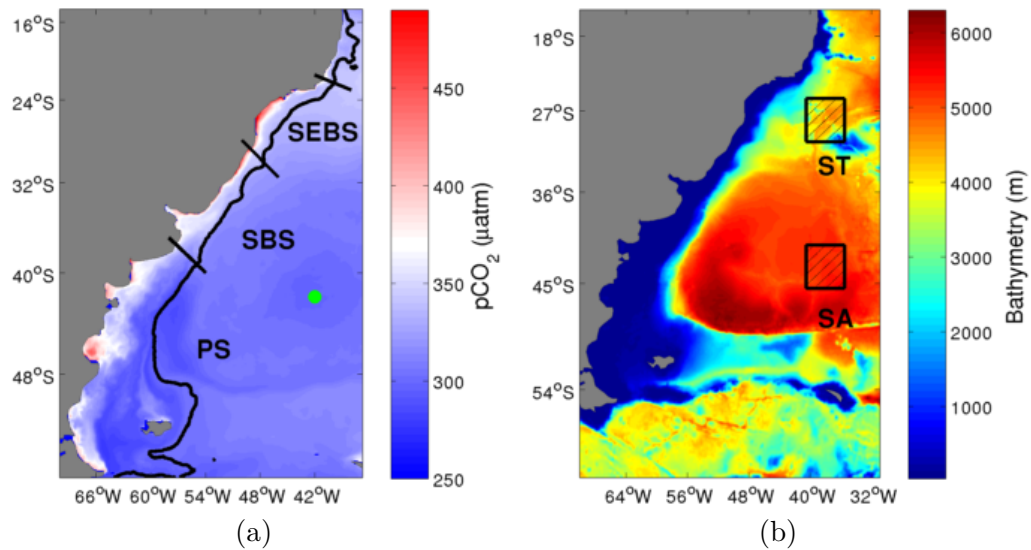


Figure 3.1: Areas utilised for the temporal analysis, (a) show the 3 continental shelves (SEBS, SBS and PS) analysed in a map with annual mean ocean surface $p\text{CO}_2$, the green circle represents the location of the vertical profile at the OOI site. (b) show the two oceanic regions (ST and SA) in a map with bathymetry.

3.3 Model Evaluation and Validation

Model results were evaluated against data from the Surface Ocean CO₂ Atlas (SOCAT) version 2 (Bakker et al., 2013). SOCAT $f\text{CO}_2$ observations were converted into $p\text{CO}_2$ using the set of equations from Körtzinger (1999) and then compared with modeled $p\text{CO}_2$ to assess the overall skill of the model. Due to the paucity of in-situ observations, particularly on the continental shelves, we used monthly climatologies for the comparison. The seasonal model evaluation was made over the whole domain (Fig.3.1). On the Patagonia Shelf, data from the Argentinian cruises ARGAU and GEF3 were used for a more focused comparison of the model results (Bianchi et al., 2009). For the Brazilian continental shelves no data were found for local comparisons.

Overall, our model represents reasonably well the seasonality of ocean surface $p\text{CO}_2$, with the latitudinal and cross-shelf gradients represented during all seasons (Fig.3.2). Since our simulation has a fixed atmospheric $p\text{CO}_2$ of 370 μatm , this value separates the source from the sink regions. In the northernmost oceanic region, between 16°S and 30°S, the observations show $p\text{CO}_2$ close to 370 – 380 μatm . Therefore this region acts as a weak source of CO₂ to the atmosphere. This

tendency is well captured by the model, particularly during summer and autumn. From 30°S to 55°S , the whole offshore region acts as a CO_2 sink, with $p\text{CO}_2$ ranging from $250\mu\text{atm}$ to $350\mu\text{atm}$ during all seasons in the model results. The observations show the same pattern down to 50°S . However in the southernmost region the observed $p\text{CO}_2$ rises to values close to $400\mu\text{atm}$. On the Southeast Brazilian Shelf, there was no data for model evaluation, but the overall behaviour of $p\text{CO}_2$ agrees with previous results from Ito et al. (2005), who suggested that the continental shelf in this region acts as a source to the atmosphere from inner to outer shelf during all seasons. The southernmost and northernmost regions are where our model has the largest biases, underestimating the ocean surface $p\text{CO}_2$. These biases could be due to a variety of reasons, including the high variability of the Antarctic Circumpolar Current and/or proximity to the model boundary with potential biases in the lateral boundary conditions used to force the model.

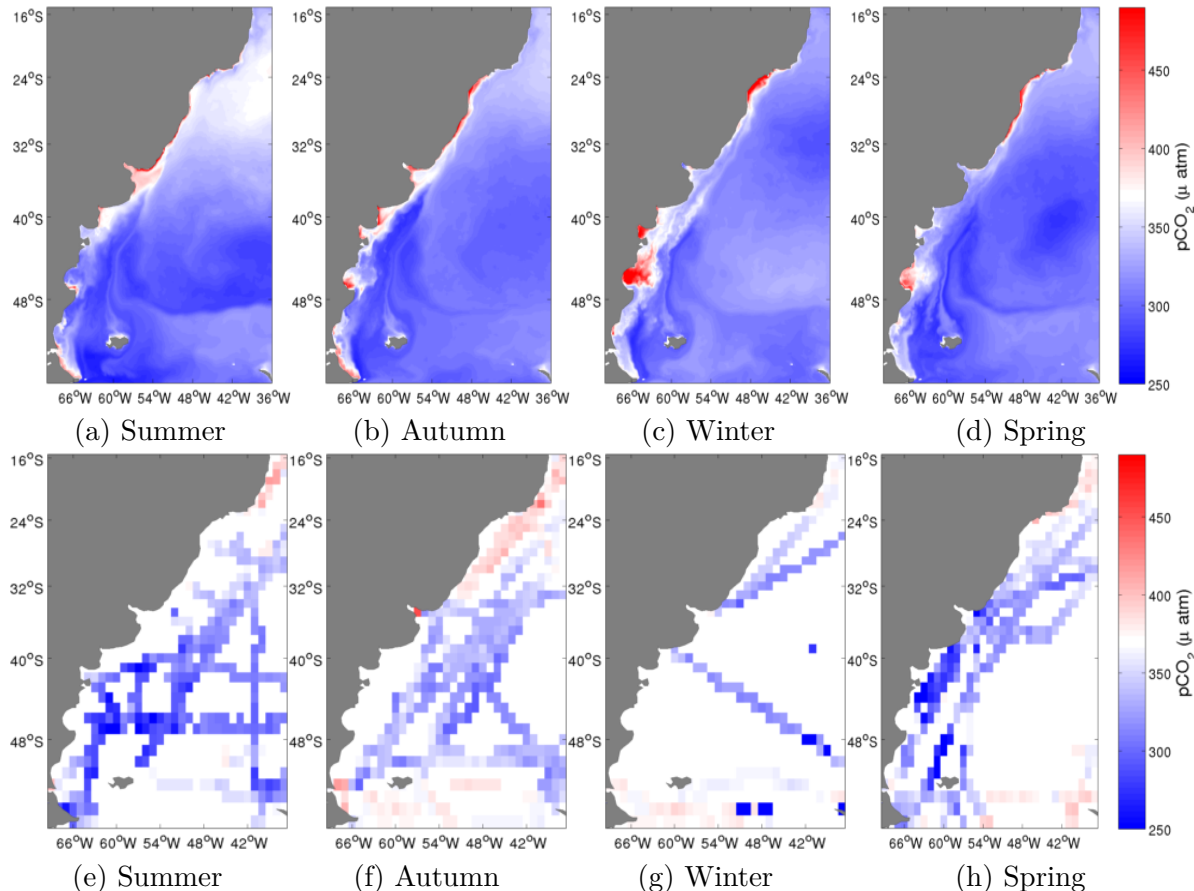


Figure 3.2: Seasonal climatology of modeled surface ocean $p\text{CO}_2$ (first row) and observations of $p\text{CO}_2$ from the SOCAT database (second row). The white separation between red and blue is set to $370\mu\text{atm}$ which is the atmospheric $p\text{CO}_2$ used in this study. Blue represent a sink of atmospheric CO_2 and red a source.

On the Patagonia Shelf the model was evaluated using in-situ observations from [Bianchi et al. \(2009\)](#) during the years 2000 to 2006 (Fig.3.3). The model agrees very well with the seasonality of the observations of this shelf region, in particular the high $p\text{CO}_2$ values along the inner shelf, characterizing these regions as a source of CO_2 during all seasons, but more intense during autumn/winter (Fig.3.3). In the mid-outer shelf the ocean generally acts as a sink, to the north the ocean is in equilibrium with the atmosphere particularly during winter.

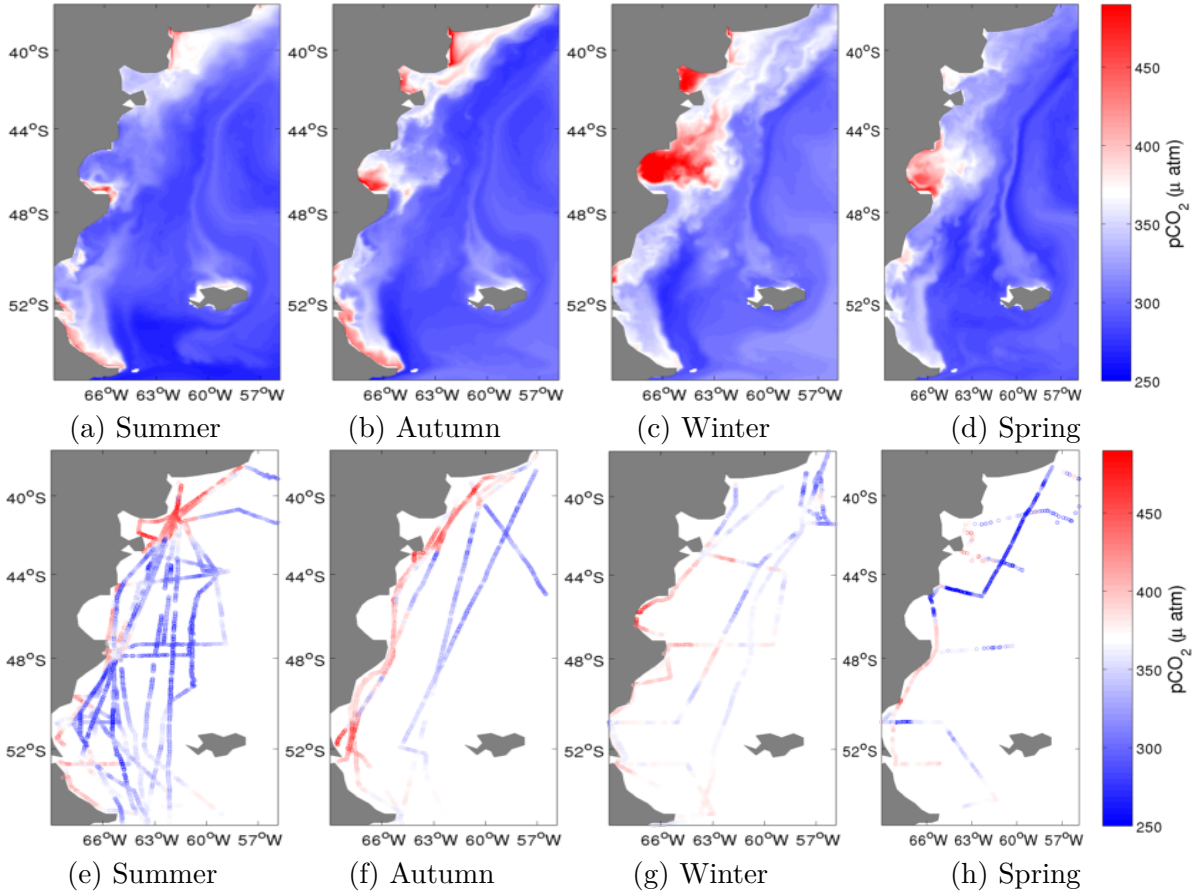


Figure 3.3: Model evaluation on the PS (zoom in from model domain in Fig. 2a). Seasonal climatology of modelled surface ocean $p\text{CO}_2$ (first row) and $p\text{CO}_2$ observations from ARGAU and GEF3 cruises(second row) ([Bianchi et al., 2009](#)). The white separation between red and blue is set to $370 \mu\text{atm}$ which is the atmospheric $p\text{CO}_2$ used in this study. Blue represent a sink of atmospheric CO_2 and red a source.

The monthly analysis was restricted to three offshore areas (A1, A2 and A3 in Fig.3.4a). We compared the spatial monthly mean modeled surface $p\text{CO}_2$ with the monthly average of the SOCAT $p\text{CO}_2$ data available in each area. Within these areas, we applied the following statistical indicators used in [Dabrowski et al. \(2014\)](#) in order to quantitatively assess model skill: model efficiency (ME) ([Nash and Sutcliffe, 1970](#)), cost function (CF) ([Ospar et al., 1998](#))

and percentage of bias (PB) (Allen et al., 2007). These statistics are indicators of the model’s performance and provide complementary information of the model skill (Dabrowski et al., 2014). Basically, $ME > 0.5$, $CF < 1$ and $PB < 20$, indicate that the model is “excellent/good”when comparing to observations.

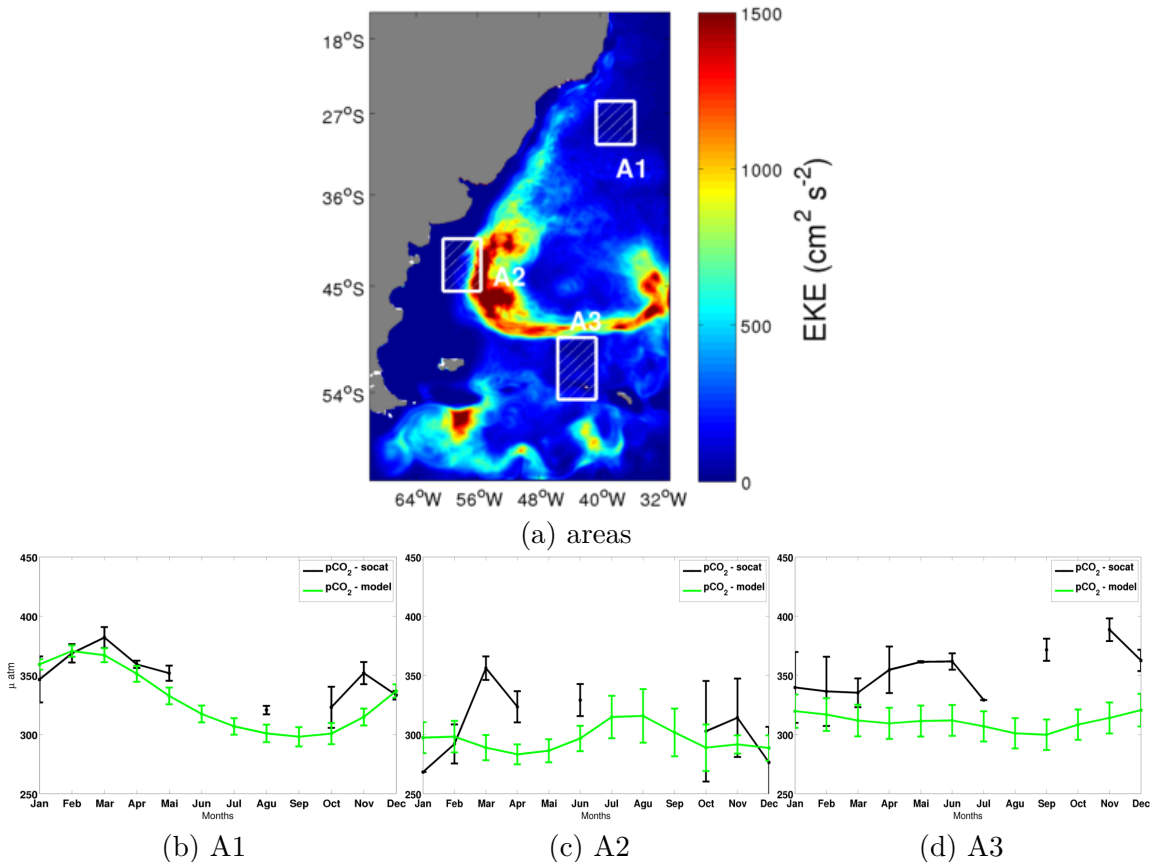


Figure 3.4: Location of the three areas used for the monthly comparison with SOCAT database (a) in a map with annual averaged eddy kinetic energy. In figures (b), (c) and (d), green lines are the modelled monthly mean $p\text{CO}_2$ and black lines are the monthly mean $p\text{CO}_2$ from SOCAT. Error bars are two standard deviations

Modeled $p\text{CO}_2$ results for A1 agree very well with the observations, representing the $p\text{CO}_2$ evolution throughout the year with maximum values in summer (Fig.3.4b). All statistical indicators characterized the model with a good/reasonable skill in A1 (Table 3.2).

A2 is the region with the largest $p\text{CO}_2$ standard deviation from both model and observations (Fig. 3.4c). This region is near the confluence between the warm Brazil Current and the cold Malvinas Current, generating one of the most energetic regions of the world’s oceans. Moreover, this region comprises the shelfbreak front, with differences in stratification, local dynamics and

salinity between shelf waters and Malvinas Current waters (Fig. 2a). Consequently, ME was estimated as poor in this region, probably due to the high $p\text{CO}_2$ data variability. But CF and PB were both rated as “reasonable/good”(Table 2).

In A3 the model consistently underestimated $p\text{CO}_2$ (Fig.3.4d). This bias is seen in the seasonal comparison and in the monthly analysis, where summer is the only season for which modelled $p\text{CO}_2$ is within the standard deviation of the observations. ME was estimated as poor in A3, but PB and CF rated our model as reasonable and good, respectively. (Table 3.2). Both A2 and A3 regions are close to an area of elevated eddy kinetic energy (Fig.3.4a), which could explain the large standard deviation and biases in these regions.

Furthermore, in order to validate the baseline of our model, seasonal climatologies of modeled sea surface temperature and chlorophyll-a were compared with climatologies from AVHRR and MODIS-aqua, respectively. Results and a detailed discussion of this validation are shown in the appendix.

Table 3.2: Statistic indicators of the model skill in the three areas (A1, A2 and A3 - Fig.3.4). Bold values indicate “good/excellent”or “reasonable”model skill when comparing to the SOCAT database.

| Area | ME | CF | PB |
|------|-------------|-------------|--------------|
| A1 | 0.23 | 0.52 | 2.88 |
| A2 | -0.18 | 0.61 | 4.23 |
| A3 | -4.70 | 1.83 | 11.59 |

In conclusion, our model reproduces satisfactorily the most important north-south and inner-outer shelf gradients seen in the $p\text{CO}_2$ observations. We now proceed to estimate the processes and drivers affecting $p\text{CO}_2$ variability in this region.

3.4 Results and Discussion

3.4.1 $p\text{CO}_2$ drivers - spatial analysis

Modeled $p\text{CO}_2$ spatial anomalies relative to the domain average are shown in Fig.3.5a, with positive anomalies on the Brazilian continental shelves, inner-mid Patagonia Shelf and North of 32°S, while the negative anomalies are in the open ocean south of 32°S and in the mid-outer

Patagonia Shelf. DIC^s has the highest impact on the spatial variations, being counteracted by ALK^s and T . (Fig.3.5). In contrast, the fresh water flux has a minor influence on the spatial anomalies of pCO_2 , agreeing with Turi et al. (2014) and Doney et al. (2009). After T and DIC^s , ALK has the larger influence on pCO_2 anomalies, with absolute values higher (-100 to $100 \mu atm$) than previous studies in other regions (Lovenduski et al., 2007; Turi et al., 2014). The higher contribution of both DIC and ALK to the spatial variations in pCO_2 could be explained by the more heterogeneous domain that encompasses several distinct surface water masses and frontal zones. Also, this elevated contribution of ALK could be due to our relatively high $CaCO_3$ to biological production ratio of 0.07.

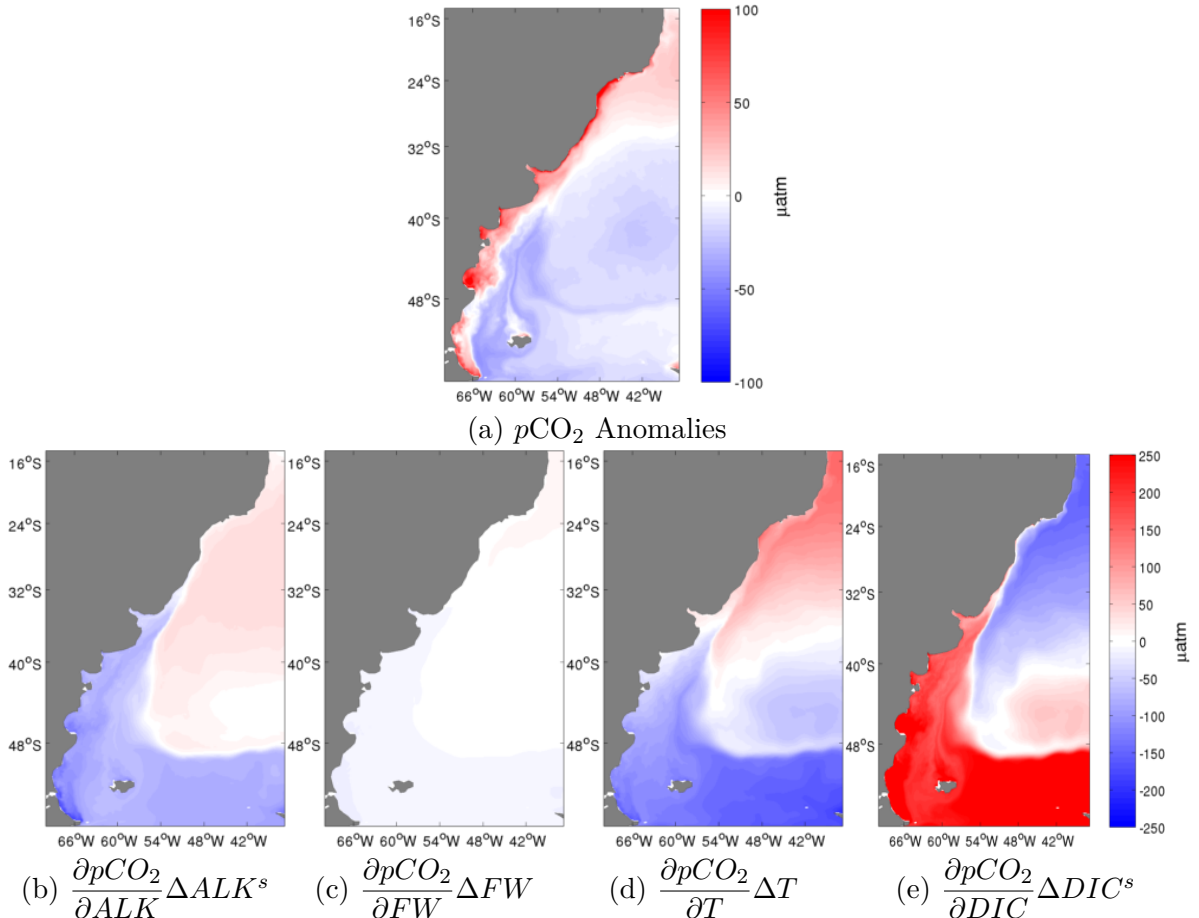


Figure 3.5: pCO_2 spatial anomalies - difference between annual mean and domain mean (a) and the contribution of the main drivers: ALK^s (b), FW (c), T (d) and DIC^s (e). Computed using spatial anomalies for Δ

The changes in the state variables affecting pCO_2 are ultimately being driven by physical and biogeochemical processes, we thus investigate which of these processes control the changes in surface pCO_2 from our sensitivity experiments (E1, E2, E3). The most important processes

affecting $p\text{CO}_2$ spatial distribution are biological production (E1 - E2) and physical transport (E3) (Fig.3.6). When physical transport (vertical and horizontal) is the only process altering $p\text{CO}_2$, we observe an increase in $p\text{CO}_2$ of up to $800\mu\text{atm}$ on the continental shelves, due to the upwelling and vertical mixing of *DIC*-rich subsurface waters. At the same time, the effect of biological production on the uptake of *DIC* and changes in *ALK* due to nitrate uptake and production/dissolution of CaCO_3 accounts for a decrease of up to $-600\mu\text{atm}$ on the continental shelves. Solubility effects (E2 - E3) are responsible for a decrease in $p\text{CO}_2$ south of 45°S and an increase in $p\text{CO}_2$ to the north, ranging from -50 to $50\mu\text{atm}$. Finally, air-sea CO_2 fluxes (Control - E1) have little impact on regulating the ocean surface $p\text{CO}_2$. The effect of both biological production and physical transport is maximal on the continental shelves, with the balance between these processes largely controlling $p\text{CO}_2$. On the open ocean north of 45°S , biological production is being counteracted by physical transport and solubility, whereas to the south of 45°S physical transport is being counteracted by biological production and solubility.

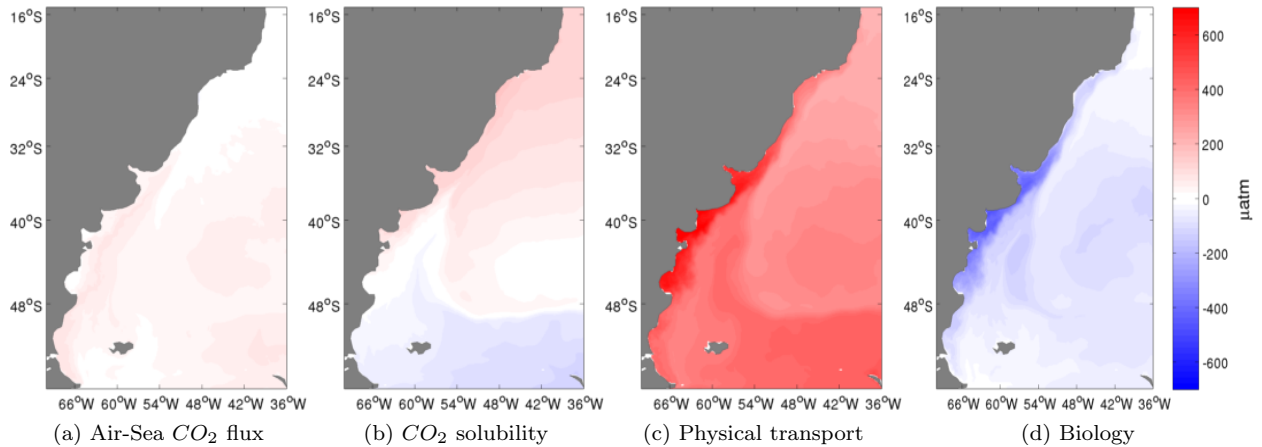


Figure 3.6: Processes driving the annual mean surface $p\text{CO}_2$. Contribution of Air-sea flux of CO_2 [Control - E1] (a), CO_2 solubility [E2 - E3] (b), physical transport [E3] (c) and biological production [E1 - E2] (d)

The strong effect of biological production on the shelf region is a result of the elevated nutrient supply and high primary production found in these regions, with increasing contribution towards the inner shelves. Physical transport presents a higher contribution on the continental shelves, where the mixed layer often spans the entire water column, showing the importance of vertical mixing in bringing metabolic *DIC* as well as nutrients to the surface waters, therefore increasing $p\text{CO}_2$. These results are in agreement with previous studies (c.f. [Turi et al. \(2014\)](#)), showing the importance of the biological net community production and advection of *ALK* and

DIC (physical transport) in controlling ocean surface pCO_2 . This suggests a major role of net community production in reducing ocean pCO_2 in the region.

3.4.2 pCO_2 drivers - temporal analysis

In order to identify the seasonal variability of the contribution of each driver, we used local grid anomalies in time over the seasonal cycle (Fig.3.7). DIC^s and T are still the most influential drivers, with increasing importance on the continental shelves. The contribution by ALK^s appears only on continental shelves south of $32^\circ S$, and FW is a minor influence (not shown). It is important to highlight that the magnitude of the signals seen in this analysis is one order of magnitude smaller than the previous spatial analysis. Thus, the high absolute contributions found in the spatial analysis are due to our large and heterogeneous domain.

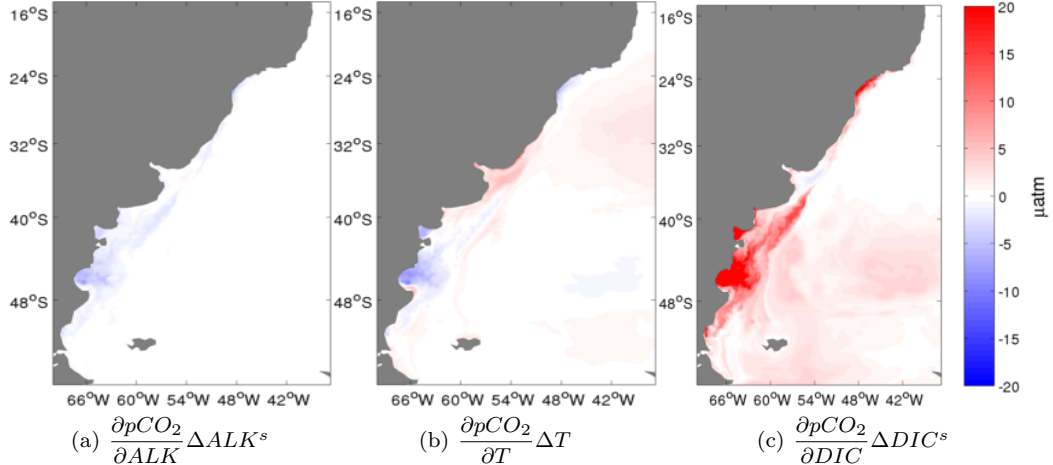


Figure 3.7: Sensitivity of pCO_2 computed with grid point anomalies in time to local annual means. Annual average contribution of the main drivers: ALK^s (a), T (b) and DIC^s (c).

The contribution of the state variables in each continental shelf region (Fig.3.8) shows that these three regions have distinct characteristics, with different contributions from each driver. In all three regions, DIC^s and T are the most important drivers of pCO_2 anomalies, albeit with opposing and seasonally varying contributions. While in summer the T contribution increases pCO_2 , that of DIC acts to diminish pCO_2 . The opposite occurs in winter. The Southeast Brazilian Shelf (SEBS) is the region with the least variability in pCO_2 anomalies, with the contributions of both DIC^s and T in this region ranging from $-10\mu\text{atm}$ to $10\mu\text{atm}$.

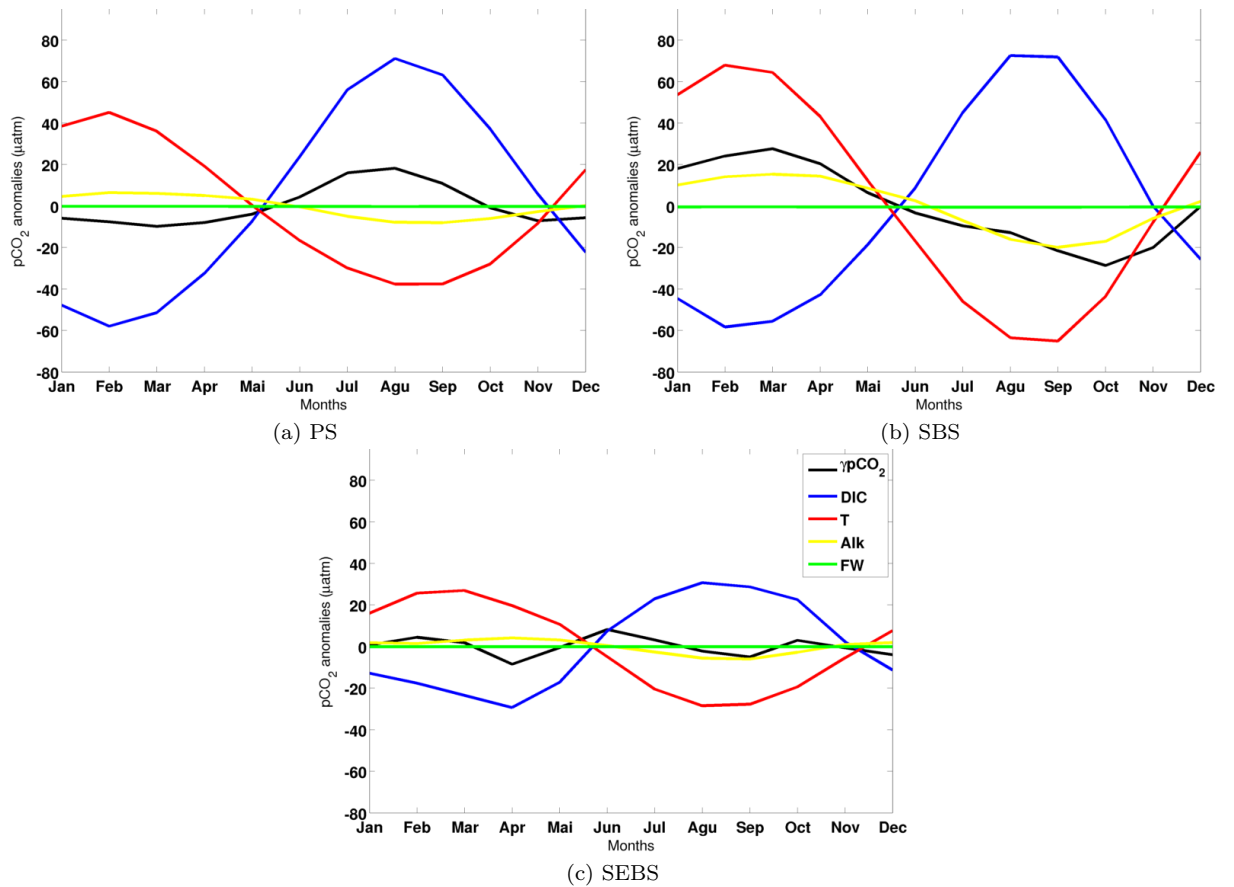


Figure 3.8: Temporal evolution of pCO_2 anomalies and their drivers in each continental shelf (right hand side of Eq. 1 using monthly anomalies), red line represents the effects of Temperature, blue line the effects of DIC^s , green line FW, and yellow line ALK^s .

The South Brazilian Shelf (SBS) is the region with the largest variability in $p\text{CO}_2$ anomalies, with ALK^s having the most prominent impact on $p\text{CO}_2$ when compared to the other regions - up to $15\mu\text{atm}$ in spring. DIC^s is the most important driver in this area, with a contribution of up to $70\mu\text{atm}$, followed by temperature, with a contribution of up to $60\mu\text{atm}$ in the winter. On the Patagonia Shelf (PS) and South Brazilian Shelf (SBS), although the amplitude of the contributions by DIC^s and T are large, the tendency of these two terms to cancel each other out results in smaller $p\text{CO}_2$ anomalies. In both SBS and PS, $p\text{CO}_2$ is predominately controlled by T and DIC^s , with small contributions from ALK and FW.

Seasonal warming/cooling is largely controlling $p\text{CO}_2$ anomalies signals throughout the continental shelves, only being damped by DIC^s , and also by ALK^s in the case of the South Brazilian Shelf (SBS). This pattern of seasonal variation of the drivers on continental shelves agrees with the results from [Signorini et al. \(2013\)](#) and [Turi et al. \(2014\)](#), although with different absolute values. Also the pattern of diminishing variability towards subtropical continental shelves is also shown by [Signorini et al. \(2013\)](#).

This pattern of opposing contributions of T and DIC was also found along the North American east coast by [Signorini et al. \(2013\)](#), who attributed winter mixing and the spring-summer biological drawdown as the processes responsible for $p\text{CO}_2$ and DIC variability. In the offshore subtropical region (ST) the $p\text{CO}_2$ anomalies have higher amplitude than in the adjacent continental shelf (SEBS), and are driven mainly by temperature, with the other variables having minor contributions (Fig.3.10). In the offshore southern region (SA), DIC controls $p\text{CO}_2$ variability, with T and ALK dampening $p\text{CO}_2$ anomalies (Fig.3.9), similar to the adjacent shelf (PS).

The analysis of the processes underlying this seasonal variability using our progressive sensitivity simulations show that on all shelf regions, biological production and CO_2 solubility mostly control $p\text{CO}_2$ variability (Fig.3.9). Physical transport, although weaker than biological production, acts to diminish the $p\text{CO}_2$ variability by counteracting the effects of biology and increasing DIC concentrations. In our case, physical transport controls $p\text{CO}_2$ spatially, but the temporal effects of physical transport are much weaker than in [Turi et al. \(2014\)](#) along the California coast. This is probably because the much stronger upwelling in that region acts to dampen the effects of biology by bringing DIC rich waters to the surface. Along western boundaries,

upwelling is weaker and more localized. Physical transport is therefore more related to processes that modulate vertical mixing and stratification, thereby controlling the seasonal enrichment of surface waters, and horizontal advection due to the presence of two major western boundary currents. Finally, air-sea CO₂ fluxes are only a minor contribution to the pCO₂ anomalies.

In conclusion, on the Patagonia Shelf (PS), the biological production is the most important contributor to pCO₂ variability, with a peak summer contribution of $-80\mu atm$ and a maximum in the winter of $70\mu atm$. On the South Brazilian Shelf (SBS), solubility is the most influential process (up to $90\mu atm$), followed by biological production and physical transport, during all seasons. On the Southeast Brazilian Shelf (SEBS), the pattern is the same as in the SBS, although with a smaller magnitude and variability. Physical transport, although large in absolute contributions in the spatial analysis, has a lower contribution to pCO₂ variability in the temporal analysis.

In the subtropical region, processes that control pCO₂ on the shelf and offshore are different. In the open ocean (ST) (Fig.3.10) pCO₂ is mainly controlled by solubility, with the biological production having the least effect on pCO₂. This contrasts with the importance of biology on mid/low latitude continental shelves (SEBS). In the subantarctic region, the processes controlling pCO₂ are similar for both the offshore region (SA) and the adjacent continental shelf (PS) (Fig.3.9). In this case biological production is the most important process being countered mainly by solubility, although with a smaller magnitude in the offshore region.

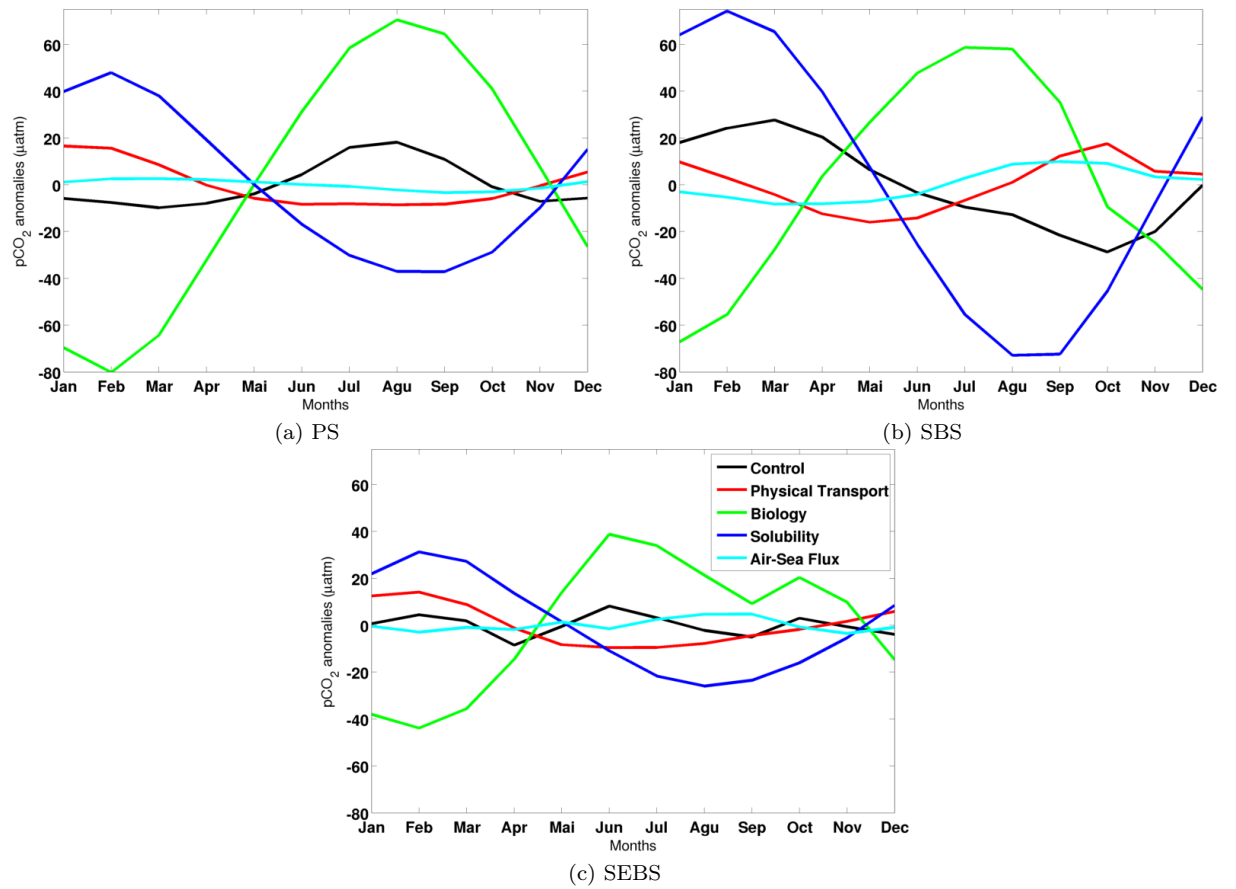


Figure 3.9: temporal evolution of the monthly anomalies of each process in regulating $p\text{CO}_2$ anomalies, green line represents the biological production, red line the physical transport, light blue line the air-sea CO_2 fluxes and dark blue line the solubility. Black lines represent the temporal $p\text{CO}_2$ anomalies.

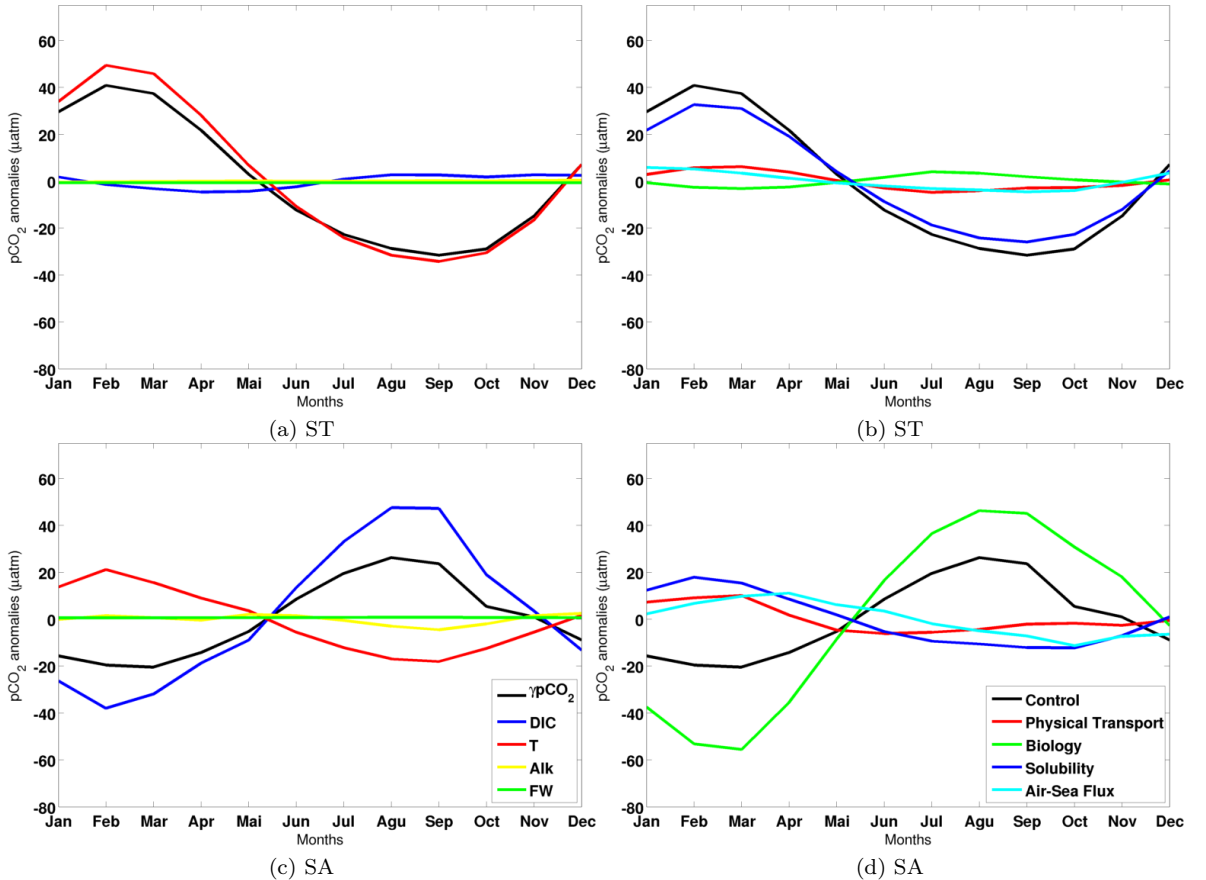


Figure 3.10: Figures (a) and (b) show the temporal evolution of $p\text{CO}_2$ anomalies and its drivers in each oceanic regions (ST and SA) (right hand side of Eq. 1 using monthly anomalies), red line represents the effects of T , blue line the effects of DIC^s , green line the FW and yellow line ALK^s . Figures (c), and (e) show the temporal evolution of the monthly anomalies of each process in regulating temporal $p\text{CO}_2$ anomalies, green line represents the biological production, red line the physical transport, light blue line the air-sea CO_2 fluxes and dark blue line the solubility. Black lines represent the temporal $p\text{CO}_2$ anomalies.

3.4.3 Air-sea CO_2 fluxes

On the continental margins, we investigate monthly averaged air-sea CO_2 fluxes on the inner shelf (0-100 meters depth), mid-outer shelf (100-200 meters depth) and shelf break-slope (200-1000 meters depth). As shown in the previous sections, the inner shelves have a potential to act as a source of CO_2 , while the mid/outer shelves tend to act as a sink of CO_2 . On the Brazilian shelves (SBS and SEBS) the flux density of CO_2 in the inner shelves is around $0 - 0.5 \text{ molCm}^{-2}\text{yr}^{-1}$, thus characterizing this region as a weak source. On the mid/outer shelf these regions shift to sinks of CO_2 , with a flux density of $-1 - 0 \text{ molCm}^{-2}\text{yr}^{-1}$ on the Southeast Brazilian shelf (SEBS). On the mid/outer South Brazilian Shelf (SBS) the sink is slightly stronger with an average flux between -1.5 and $-0.5 \text{ molCm}^{-2}\text{yr}^{-1}$ (Figs. 3.11a and 3.11b). The Patagonia Shelf (PS) acts on average as a sink of CO_2 , with fluxes larger than on the Brazilian shelves. CO_2 absorption on PS intensifies from the inner shelf ($-1.0 / -0.5 \text{ molCm}^{-2}\text{yr}^{-1}$) to the outer shelf and continental slope ($-2.0 / -4.0 \text{ molCm}^{-2}\text{yr}^{-1}$) (Fig. 3.11c). Although, PS acts on average as a sink throughout the whole continental shelf, there are some coastal regions that act as a source of CO_2 , which agrees with the observations of [Bianchi et al. \(2009\)](#).

Annual averaged modelled air-sea CO_2 fluxes agreed reasonably well with global climatologies in the oceanic regions (not shown) ([Takahashi et al., 2002](#); [Landschützer et al., 2014](#)). South of $30^\circ S$, the open ocean acts on average as a sink of atmospheric CO_2 , absorbing up to $4\text{molCm}^{-2}\text{yr}^{-1}$. North of $30^\circ S$, the open ocean is on average in equilibrium with the atmosphere (Fig. 3.10). On the continental margins, our annual averaged air-sea CO_2 fluxes compares well with the global estimate from [Laruelle et al. \(2014\)](#), where the Patagonian Shelf acts as a sink of CO_2 (-1.0 to $-4.0 \text{ molCm}^{-2}\text{yr}^{-1}$) and the Brazilian shelves act as a weak source of CO_2 (0 to $1 \text{ molCm}^{-2}\text{yr}^{-1}$). Nevertheless, we found variability on each continental shelf, with regions on the inner Patagonia Shelf acting as a source or in equilibrium with the atmosphere (0 to $2.0 \text{ molCm}^{-2}\text{yr}^{-1}$), and regions on the outer Brazilian shelves acting as a sink of CO_2 .

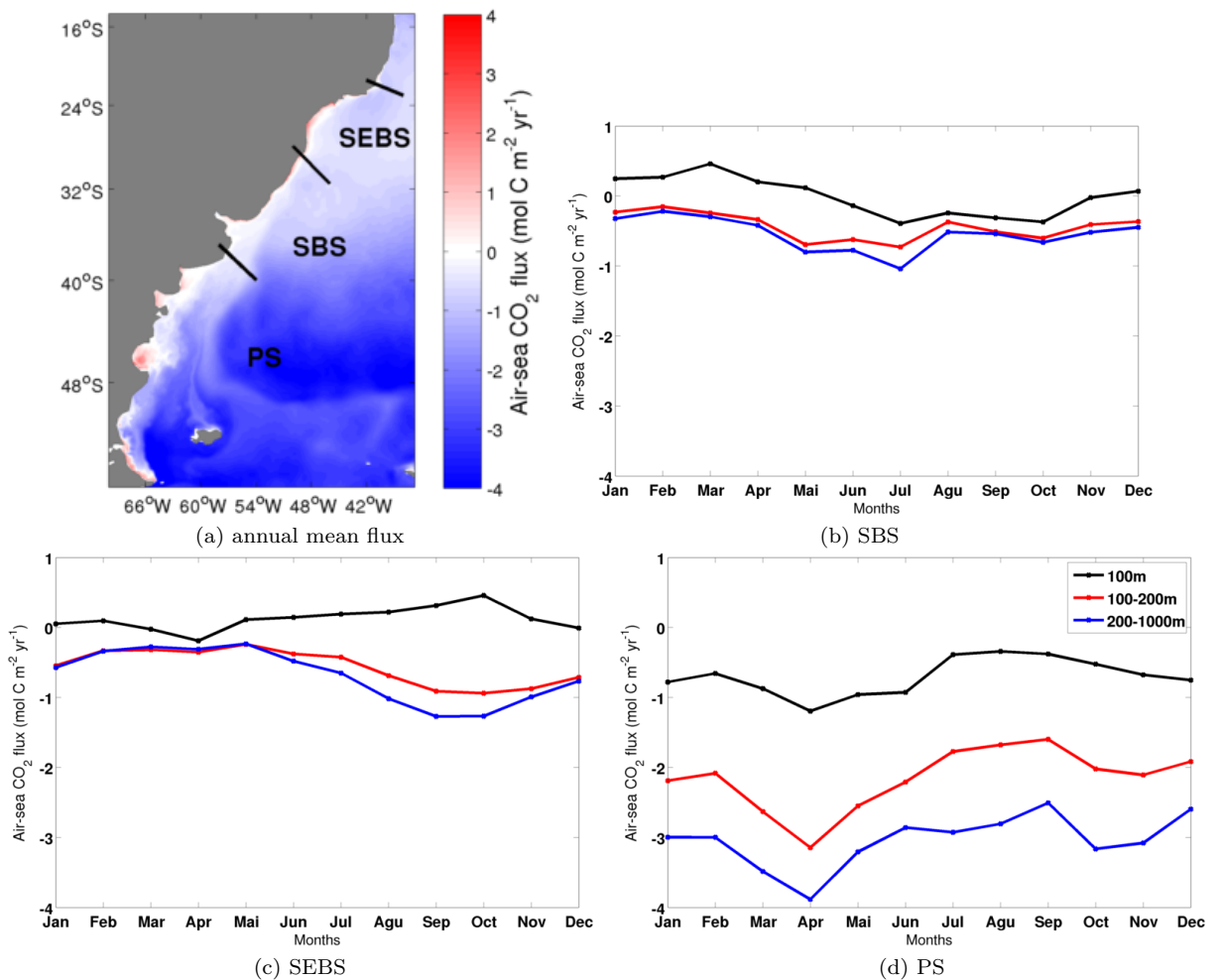


Figure 3.11: Figure (a) is the annual average of air-sea CO_2 fluxes. Figures (b), (c) and (d) show the monthly average of surface CO_2 fluxes constrained to bathymetry levels of 100m, 200m and 1000m.

3.4.4 Vertical Structure - Case Study at Argentine OOI Site

Seasonal variations in mixing and stratification control the evolution of the mixed layer depth and consequently the vertical structure of the state variables of the carbonate system. Diapycnal fluxes of DIC and DIC sinks from primary production are important processes regulating ocean surface pCO_2 (Rippeth et al., 2014). Therefore, the mixed layer depth is linked with the surface pCO_2 variability.

In order to understand the seasonal evolution of the upper ocean vertical distribution of the state variables in the region and how it affects surface pCO_2 , we chose the location of the Ocean Observatory Initiative (OOI) site in the Argentine Basin at $42^\circ S$, $42^\circ W$, as it will soon become a test-bed for the validation of biogeochemical models globally and regionally. We extracted modeled climatological vertical profiles of DIC concentration, temperature and chlorophyll-a, and compared with the modelled surface pCO_2 and mixed layer depth (Fig.3.12).

During the entire year, this location acts in our model as a sink for atmospheric CO_2 , with modelled surface pCO_2 ranging from $280\mu atm$ to $320\mu atm$. The contribution of DIC^s and T are again driving surface pCO_2 anomalies. In this case DIC^s is controlling the anomalies signal, being dampened by temperature. The main processes affecting pCO_2 in this location is biological production and solubility. Minimum pCO_2 in summer coincides with strong stratification and elevated subsurface biological production, respectively, with the opposing contribution of DIC^s and T leading to pCO_2 anomalies near zero. Maximum pCO_2 occurs when the mixed layer depth deepens, during fall and winter, when vertical mixing cause an increase in the concentration of DIC in the surface waters. This affects pCO_2 much more than the decrease in temperature, resulting in positive pCO_2 anomalies. After winter, this excess of DIC is consumed by biological fixation during spring and summer, thus reducing surface pCO_2 .

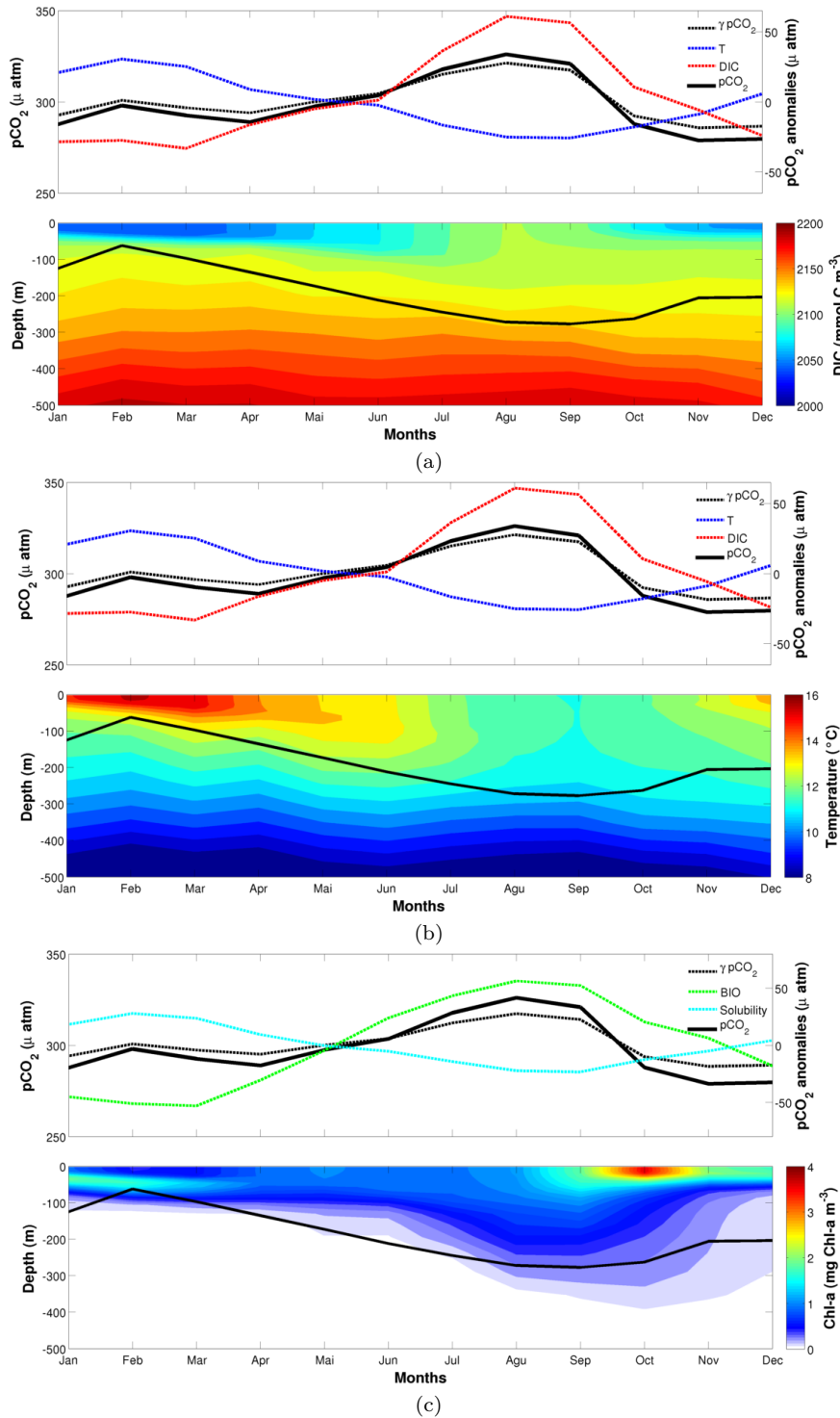


Figure 3.12: Vertical profile at 42° S, 42° W , upper panels showing monthly mean surface $p\text{CO}_2$ (solid black line), $p\text{CO}_2$ anomalies (dashed black line) and the contribution from the main drivers (Fig. (a) and (b)) and the main processes (Fig. (c)). Lower panels showing vertical profiles of DIC (a), T (b), and chlorophyll concentration (c), black line represents the mixed layer depth.

3.5 Conclusions

In this study, we used a regional hydrodynamical model coupled with a biogeochemical model to investigate, in a climatological sense, the main drivers and processes that control ocean surface $p\text{CO}_2$ and air-sea CO_2 fluxes in the southwestern Atlantic Ocean. Modeled ocean surface $p\text{CO}_2$ compared well with the available in-situ data, reproducing the expected meridional and cross-shelf gradients of $p\text{CO}_2$, with elevated $p\text{CO}_2$ in the inner shelves and at lower latitudes. Our results highlight that the most important variables controlling the spatio-temporal variability of $p\text{CO}_2$ are T and DIC . These two variables have opposing effects on $p\text{CO}_2$ and have been shown to be the main drivers of $p\text{CO}_2$ both in global (Sarmiento and Gruber, 2006; Doney et al., 2009) and in other regional studies (Turi et al., 2014; Signorini et al., 2013; Lovenduski et al., 2007). Following DIC and T , we found that ALK is an important spatial regulator of $p\text{CO}_2$, with increasing importance on the South Brazilian Shelf (SBS) and in the southern open ocean region (SA).

The most important processes underlying changes on the state variables and thus on $p\text{CO}_2$ are biological production and CO_2 solubility. Biological production is particularly important on the continental shelves, with higher contribution towards continental shelves at high latitudes. On the open ocean, solubility is the main processes driving $p\text{CO}_2$ in the subtropics, while in the sub-antarctic both CO_2 solubility and biological production are important drivers of $p\text{CO}_2$ variability.

The southwestern Atlantic Ocean acts, on average, as sink of atmospheric CO_2 south of $30^\circ S$, and is close to equilibrium to the north. In the inner continental shelves the ocean acts either as a weak source or is in equilibrium with the atmosphere. To the outer shelf the ocean shifts to a sink of CO_2 . The entire Patagonian shelf acts, on average, as a sink, but there are some particular regions in the inner shelf that acts as a source of CO_2 . The total integrated flux agrees well with Laruelle et al. (2014), particularly on the Brazilian Shelves (SEBS and SBS). However, in the Patagonia Shelf (PS), we found a slightly stronger sink on the mid/outer Patagonian Shelf (-1.0 to $-4.0 \text{ molCm}^{-2}\text{yr}^{-1}$) and more variability towards the inner shelf.

Modelling studies such as this one depend heavily on in-situ observations, the lack of which hampers our ability to properly refine our model, this will certainly be improved by future efforts

of data assimilation of vertical profiles of biogeochemical and physical variables from the OOI site at the Argentine basin. In future studies we will also add tides and river run-off to the model, hopefully diminishing the biases in the southernmost and La Plata regions. However, this study is a first step in understanding the processes controlling surface $p\text{CO}_2$ in an undersampled, yet highly important, region of the world's ocean. Improved understanding of the processes controlling the surface distribution of $p\text{CO}_2$ on continental shelves and open ocean is fundamental for quantifying the ocean's response to and its feedback on climate change.

3.6 Appendix - Model Validation (SST and Chlorophyll-a)

Seasonal climatologies of 4 years of modeled sea surface temperature and chlorophyll-a concentration were compared with climatologies from the sensors AVHRR (1985-2002) and Modis-aqua (2003-2013), respectively (Figs. 3.13 and 3.14). Modeled sea surface temperature compared well with AVHRR (Fig.3.13) representing both subantarctic and subtropical oceanic regions during all seasons.

Modeled chlorophyll-a concentration reproduces the general pattern from MODIS-aqua (Fig.3.14), with low concentrations in the oceanic regions and higher concentrations on the continental shelves. However, modeled chlorophyll-a concentrations are overestimated in the oceanic regions ($0.5 \text{ mgChla} - \text{am}^{-3}$), especially in the spring season (up to $1 \text{ mgChla} - \text{am}^{-3}$). On the coastal regions, we underestimate chlorophyll-a on the Patagonia Shelf during spring and summer seasons. Expectedly, there was an underestimation in the La Plata region, since we are not modeling the nutrient and organic loads from the river. Finally, on the Brazilian shelf our model overestimates chlorophyll-a, particularly during summer and spring seasons. These biases may be due to our application of a relatively simple ecosystem model with only one phytoplankton functional type in such a wide region, which encompasses several ecological provinces. Nevertheless, the general pattern is well reproduced in this first effort in modeling the biogeochemistry of the southwestern Atlantic Ocean, and the biases may not significantly compromise our analysis of drivers and processes on $p\text{CO}_2$ variability.

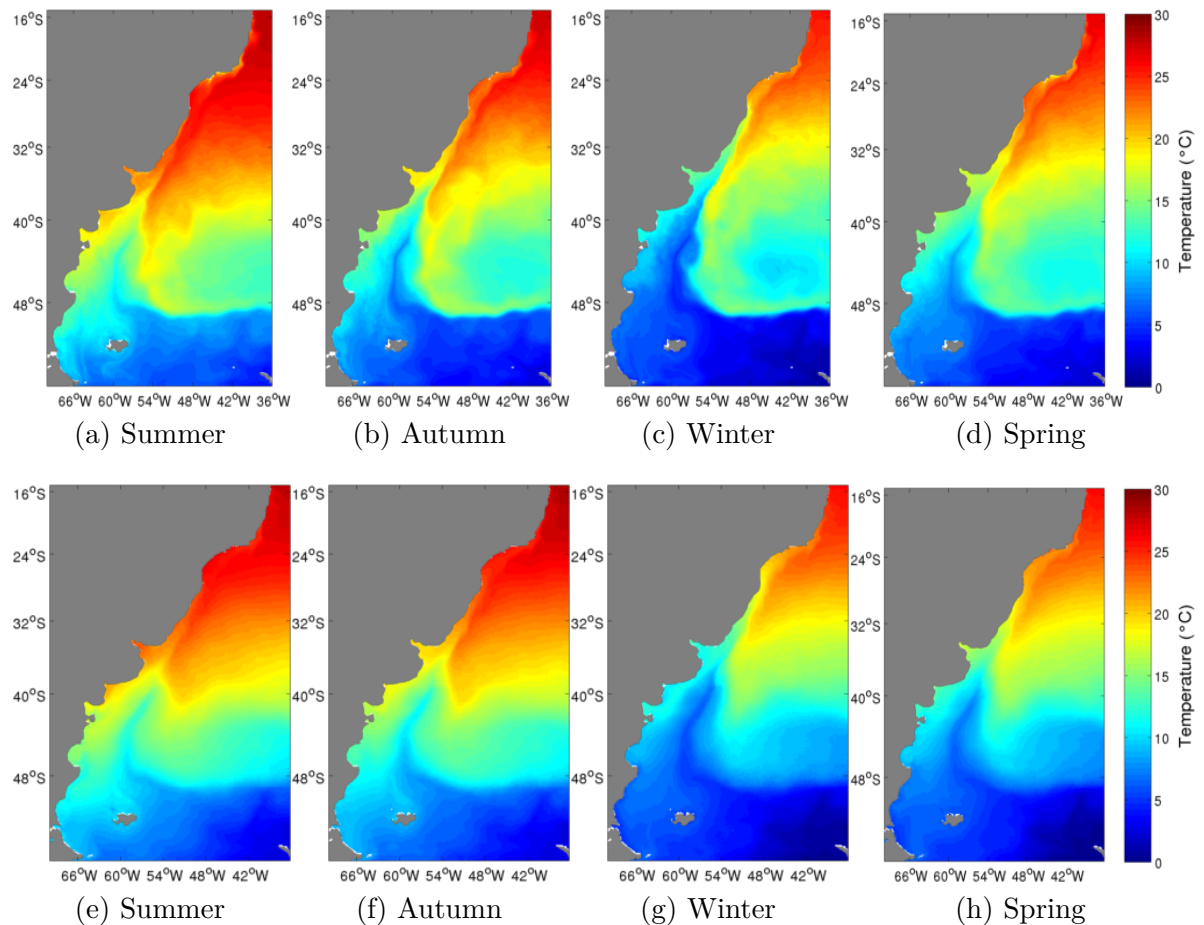


Figure 3.13: Seasonal climatology of modeled sea surface temperature $^{\circ}\text{C}$ - 4 years average (first row), and climatology from AVHRR sensor - from 1985 to 2002 (second row).

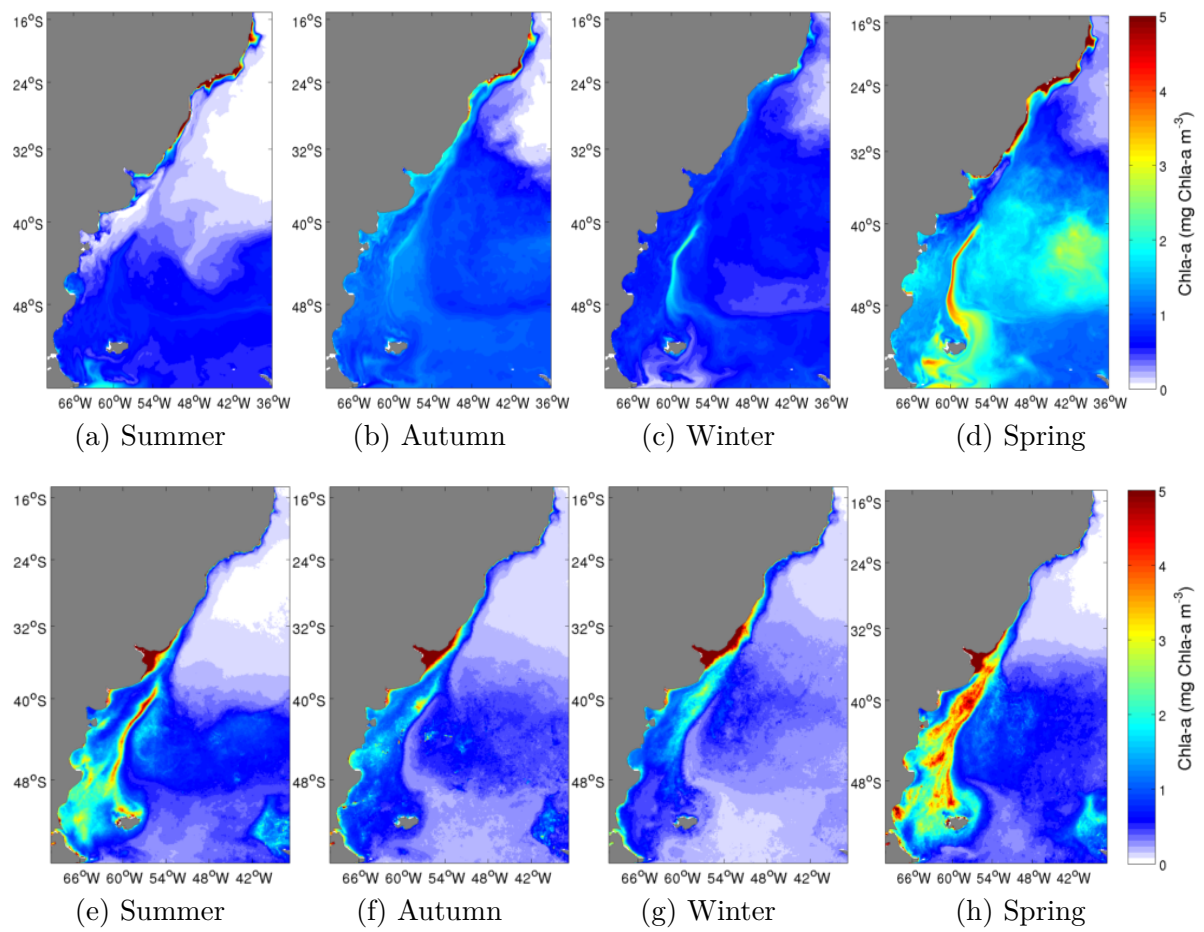


Figure 3.14: Seasonal climatology of modeled chlorophyll-a concentration $mgChla - am^{-3}$ - 4 years average (first row), and climatology from Aqua-Modis sensor - from 2003 to 2013 (second row).

3.7 acknowledgments

PHRC acknowledges support from the Brazilian agencies Conselho Nacional de Desenvolvimento Científico e Tecnológico (CNPq), grants 483112/2012-7 and 307385/2013-2, and the Fundação de Amparo a Pesquisa do Estado do Rio Grande do Sul (FAPERGS), grant 2166/12-8. RA acknowledges support from a CAPES scholarship. SCD and IDL acknowledge support from the National Science Foundation (NSF AGS-1048827). NG and GT received support from ETH Zurich and from the EU FP7 project CarboChange (264879).

The Surface Ocean CO₂ Atlas (SOCAT) is an international effort, supported by the International Ocean Carbon Coordination Project (IOCCP), the Surface Ocean Lower Atmosphere Study (SOLAS), and the Integrated Marine Biogeochemistry and Ecosystem Research program (IMBER), to deliver a uniformly quality-controlled surface ocean CO₂ database. The many researchers and funding agencies responsible for the collection of data and quality control are thanked for their contributions to SOCAT.

We are greatly indebted with the Ministero de Defensa de Argentina that supported the project “Balance y variabilidad del flujo mar-aire en el Mar Patagónico”(PIDDEF 47/11).

Capítulo

4

Considerações Finais

Este trabalho apresentou uma análise dos fluxos líquidos de CO₂ e dos principais controladores da variabilidade do *pCO₂* superficial no Oceano Atlântico Sudoeste. Através de modelagem numérica biogeoquímica, os resultados de *pCO₂* obtidos neste estudo climatológico reproduziram o padrão encontrado nas observações. Na média, em todas as plataformas continentais há um gradiente de *pCO₂*, apresentando elevados valores de *pCO₂* nas plataformas internas e regiões oceânicas de baixa latitude, caracterizando essas regiões como fonte de CO₂ para atmosfera, e baixos valores de *pCO₂* nas plataformas médias e externas, e regiões oceânicas de médias/altas latitudes, caracterizando essas regiões como sumidouros de CO₂ atmosférico.

A variabilidade temporal do *pCO₂* aumenta com a latitude, a Plataforma Sudeste Brasileira foi a região com menores anomalias temporais. As principais variáveis controlando as anomalias espaço-temporal de *pCO₂* são *DIC* e temperatura. Essas duas variáveis possuem efeitos opostos no *pCO₂*, e são os principais controladores tanto em plataforma continental quanto *offshore*. A alcalinidade apresentou-se como a terceira variável mais importante, principalmente na Plataforma Sul Brasileira. Já o fluxo de água doce apresentou impacto minoritário no *pCO₂*.

Os processos que mais afetam as variáveis de estado, e consequentemente o *pCO₂*, são a produção biológica e a solubilidade do CO₂. O transporte físico apresentou importância somente na análise espacial, enquanto o impacto dos fluxos de CO₂ apresentaram apenas impacto minoritário no *pCO₂*. A produção biológica apresenta maior contribuição nas plataformas e regiões oceânicas de médias latitudes, enquanto na região oceânica subtropical o *pCO₂* é controlado quase que exclusivamente pela solubilidade do CO₂. O comportamento da Plataforma da Patago-

nia apresenta um comportamento similar com o oceano adjacente, sendo controlado por ambos os processos de produção biológica e solubilidade, no entanto a produção biológica apresenta maiores magnitudes na plataforma.

As plataformas médias e externas, caracterizadas como sumidouros de carbono atmosférico, apresentam um potencial para o bombeamento de carbono das plataformas para o oceano adjacente. Para estudos futuros, a quantificação dos fluxos horizontais de *DIC* em profundidades superiores a camada de mistura serão importantes estimativas da bomba de carbono da plataforma nessas regiões. Além disso, sugere-se a implementação de marés e de aporte fluvial de carbono orgânico e inorgânico no Rio da Prata, ambos esses processos são importantes localmente para a variabilidade de $p\text{CO}_2$.

Este estudo é o início para a modelagem biogeoquímica do $p\text{CO}_2$ no Atlântico Sudoeste. Estudos de modelagem numérica são dependentes de observações in-situ, com o aumento da densidade de dados observacionais o modelo biogeoquímico poderá ser refinado. Foi apresentado uma abordagem climatológica para que essa investigação possa servir de linha de base para futuras estimativas. O conhecimento das variáveis e processos controladores das anomalias de $p\text{CO}_2$ apresenta importância devido à elevada incerteza do papel das plataformas continentais no ciclo do carbono global, e é fundamental para quantificar a resposta dos oceanos às mudanças climáticas.

Bibliografia

- Allen, J., Somerfield, P., and Gilbert, F. (2007). Quantifying uncertainty in high-resolution coupled hydrodynamic-ecosystem models. *Journal of Marine Systems*, 64(1-4):3–14.
- Bakker, D. C. E., Pfeil, B., Smith, K., Hankin, S., Olsen, a., Alin, S. R., Cosca, C., Harasawa, S., Kozyr, a., Nojiri, Y., O’Brien, K. M., Schuster, U., Telszewski, M., Tilbrook, B., Wada, C., Akle, J., Barbero, L., Bates, N., Boutin, J., Cai, W.-J., Castle, R. D., Chavez, F. P., Chen, L., Chierici, M., Currie, K., de Baar, H. J. W., Evans, W., Feely, R. a., Fransson, a., Gao, Z., Hales, B., Hardman-Mountford, N., Hoppema, M., Huang, W.-J., Hunt, C. W., Huss, B., Ichikawa, T., Johannessen, T., Jones, E. M., Jones, S. D., Jutterström, S., Kitidis, V., Kötzinger, a., Landschtzer, P., Lauvset, S. K., Lefèvre, N., Manke, a. B., Mathis, J. T., Merlivat, L., Metzl, N., Murata, a., Newberger, T., Ono, T., Park, G.-H., Paterson, K., Pierrot, D., Ríos, a. F., Sabine, C. L., Saito, S., Salisbury, J., Sarma, V. V. S. S., Schlitzer, R., Sieger, R., Skjelvan, I., Steinhoff, T., Sullivan, K., Sun, H., Sutton, a. J., Suzuki, T., Sweeney, C., Takahashi, T., Tjiputra, J., Tsurushima, N., van Heuven, S. M. a. C., Vandemark, D., Vlahos, P., Wallace, D. W. R., Wanninkhof, R., and Watson, a. J. (2013). An update to the Surface Ocean CO_2 Atlas (SOCAT version 2). *Earth System Science Data Discussions*, 6(2):465–512.
- Bauer, J. E., Cai, W.-J., Raymond, P. a., Bianchi, T. S., Hopkinson, C. S., and Regnier, P. a. G. (2013). The changing carbon cycle of the coastal ocean. *Nature*, 504(7478):61–70.
- Bianchi, A. a., Pino, D. R., Perlender, H. G. I., Osiroff, A. P., Segura, V., Lutz, V., Clara, M. L., Balestrini, C. F., and Piola, A. R. (2009). Annual balance and seasonal variability of sea-air CO_2 fluxes in the Patagonia Sea: Their relationship with fronts and chlorophyll distribution. *Journal of Geophysical Research*, 114(C3):C03018.
- Bianchi, A. A., Piola, A. R., Pino, D. R., Schloss, I., Poisson, A., and Balestrini, C. F. (2005).

- Vertical stratification and air-sea CO₂ fluxes in the Patagonian shelf. *Journal of Geophysical Research*, 110(C7):C07003.
- Bozec, Y., Thomas, H., Elkalay, K., and de Baar, H. J. (2005). The continental shelf pump for CO₂ in the north sea—evidence from summer observation. *Marine Chemistry*, 93(2):131–147.
- Burd, A. B., Hansell, D. A., Steinberg, D. K., Anderson, T. R., Arístegui, J., Baltar, F., Beaupre, S. R., Buesseler, K. O., DeHairs, F., Jackson, G. A., et al. (2010). Assessing the apparent imbalance between geochemical and biochemical indicators of meso-and bathypelagic biological activity: What the @#\$#! is wrong with present calculations of carbon budgets? *Deep Sea Research Part II: Topical Studies in Oceanography*, 57(16):1557–1571.
- Cai, W.-J. (2003). The role of marsh-dominated heterotrophic continental margins in transport of CO₂ between the atmosphere, the land-sea interface and the ocean. *Geophysical Research Letters*, 30(16):1849.
- Carton, J. A. and Giese, B. S. (2008). A reanalysis of ocean climate using simple ocean data assimilation (soda). *Monthly Weather Review*, 136(8):2999–3017.
- Castro, B. d. and Miranda, L. d. (1998). Physical oceanography of the western atlantic continental shelf located between 4° n and 34° s. *The sea*, 11(1):209–251.
- Chen, C.-T. a., Huang, T.-H., Chen, Y.-C., Bai, Y., He, X., and Kang, Y. (2013). Air-sea exchanges of CO₂ in world's coastal seas. *Biogeosciences Discussions*, 10(3):5041–5105.
- Christensen, J. P. (1994). Carbon export from continental shelves, denitrification and atmospheric carbon dioxide. *Continental Shelf Research*, 14(5):547–576.
- Caias, P., Sabine, C., Bala, G., Bopp, L., Brovkin, V., Canadell, J., Chhabra, A., DeFries, R., Galloway, J., Heimann, M., et al. (2014). Carbon and other biogeochemical cycles. In *Climate Change 2013: The Physical Science Basis. Contribution of Working Group I to the Fifth Assessment Report of the Intergovernmental Panel on Climate Change*, pages 465–570. Cambridge University Press.
- Ciotti, Á. M., de Mahiques, M., and Möller, O. O. (2014). The meridional gradients of the s-se brazilian continental shelf: Introduction to the special volume. *Continental Shelf Research*, 89:1–4.

- Da Silva, A., Young, C., and Levitus, S. (1994). Atlas of surface marine data 1994, vol. 1, algorithms and procedures, noaa atlas nesdis 6. *US Department of Commerce, NOAA, NESDIS, USA*, page 74.
- Dabrowski, T., Lyons, K., Berry, A., Cusack, C., and Nolan, G. D. (2014). An operational biogeochemical model of the North-East Atlantic: Model description and skill assessment. *Journal of Marine Systems*, 129:350–367.
- Doney, S. C., Lima, I., Feely, R. a., Glover, D. M., Lindsay, K., Mahowald, N., Moore, J. K., and Wanninkhof, R. (2009). Mechanisms governing interannual variability in upper-ocean inorganic carbon system and air-sea CO₂ fluxes: Physical climate and atmospheric dust. *Deep Sea Research Part II: Topical Studies in Oceanography*, 56(8-10):640–655.
- Fennel, K. (2010). The role of continental shelves in nitrogen and carbon cycling. *Ocean Science Discussions*, 7(1):177–205.
- Fennel, K. and Wilkin, J. (2009). Quantifying biological carbon export for the northwest north atlantic continental shelves. *Geophysical Research Letters*, 36(18).
- Gonzalez-Silvera, A., Santamaria-del Angela, E., Garcia, V. M. T., Garcia, C. A. E., Millan-Nunez, R., and Muller-Karger, F. (2004). Biogeographical regions of the tropical and subtropical Atlantic Ocean off South America: classification based on pigment (CZCS) and chlorophyll-a(SeaWiFS). *Continental Shelf* . . . , 24:983–1000.
- Gruber, N. (2015). Ocean biogeochemistry: Carbon at the coastal interface. *Nature*.
- Gruber, N., Frenzel, H., Doney, S. C., Marchesiello, P., McWilliams, J. C., Moisan, J. R., Oram, J. J., Plattner, G.-K., and Stolzenbach, K. D. (2006). Eddy-resolving simulation of plankton ecosystem dynamics in the California Current System. *Deep Sea Research Part I: Oceanographic Research Papers*, 53(9):1483–1516.
- Gruber, N., Lachkar, Z., Frenzel, H., Marchesiello, P., Münnich, M., McWilliams, J. C., Nagai, T., and Plattner, G.-K. (2011). Eddy-induced reduction of biological production in eastern boundary upwelling systems. *Nature Geoscience*, 4(11):787–792.
- Guerrero, R. A., Piola, A. R., Fenco, H., Matano, R. P., Combes, V., Chao, Y., James, C., Palma, E. D., Saraceno, M., and Strub, P. T. (2014). The salinity signature of the cross-shelf exchanges

- in the southwestern atlantic ocean: Satellite observations. *Journal of Geophysical Research: Oceans*, 119(11):7794–7810.
- Hauri, C., Gruber, N., Vogt, M., Doney, S. C., Feely, R. A., Lachkar, Z., Leinweber, A., McDonnell, A. M., Munnich, M., and Plattner, G.-K. (2013). Spatiotemporal variability and long-term trends of ocean acidification in the california current system.
- Hofmann, E. E., Cahill, B., Fennel, K., a.M. Friedrichs, M., Hyde, K., Lee, C., Mannino, A., Najjar, R. G., O'Reilly, J. E., Wilkin, J., and Xue, J. (2011). Modeling the Dynamics of Continental Shelf Carbon. *Annual Review of Marine Science*, 3(1):93–122.
- Ito, R., Schneider, B., and Thomas, H. (2005). Distribution of surface fCO₂ and air-sea fluxes in the Southwestern subtropical Atlantic and adjacent continental shelf. *Journal of Marine Systems*, 56(3-4):227–242.
- Kantha, L. (1995). Barotropic tides in the global oceans from a nonlinear tidal model assimilating altimetric tides: 1. Model description and results. *Journal of Geophysical Research: Oceans (1978–…)*, 100:283–308.
- Körtzinger, A. (1999). Determination of carbon dioxide partial pressure (p (co₂)). *Methods of Seawater Analysis, Third Edition*, pages 149–158.
- Lachkar, Z. and Gruber, N. (2013). Response of biological production and air-sea CO₂ fluxes to upwelling intensification in the California and Canary Current Systems. *Journal of Marine Systems*, 109-110:149–160.
- Landschützer, P., Gruber, N., Bakker, D., and Schuster, U. (2014). Recent variability of the global ocean carbon sink. *Global Biogeochemical Cycles*, 28(9):927–949.
- Laruelle, G. G., Dürr, H. H., Lauerwald, R., Hartmann, J., Slomp, C. P., Goossens, N., and Regnier, P. a. G. (2013). Global multi-scale segmentation of continental and coastal waters from the watersheds to the continental margins. *Hydrology and Earth System Sciences*, 17(5):2029–2051.
- Laruelle, G. G., Lauerwald, R., Pfeil, B., and Regnier, P. (2014). Regionalized global budget of the co₂ exchange at the air-water interface in continental shelf seas. *Global Biogeochemical Cycles*.

- Le Quéré, C., Moriarty, R., Andrew, R., Peters, G., Ciais, P., Friedlingstein, P., Jones, S., Sitch, S., Tans, P., Arneth, A., et al. (2014). Global carbon budget 2014. *Earth System Science Data Discussions*, 7(2):521–610.
- Liu, K.-K., Atkinson, L., Quiñones, R., and Talaue-McManus, L. (2010). *Carbon and nutrient fluxes in continental margins: a global synthesis*. Springer Science & Business Media.
- Longhurst, A., Sathyendranath, S., Platt, T., and Caverhill, C. (1995). An estimate of global primary production in the ocean from satellite radiometer data. *Journal of Plankton Research*, 17(6):1245–1271.
- Lovenduski, N. S., Gruber, N., Doney, S. C., and Lima, I. D. (2007). Enhanced CO₂ outgassing in the Southern Ocean from a positive phase of the Southern Annular Mode. *Global Biogeochemical Cycles*, 21(2):n/a–n/a.
- Matano, R., Palma, E., and Piola, A. (2010). The influence of the brazil and malvinas currents on the southwestern atlantic shelf circulation. *Ocean Science*, 6(4):983–995.
- Millero, F. (1995). Thermodynamics of the carbon dioxide system in the oceans. *Geochimica et Cosmochimica Acta*, 59(4):661–677.
- Muller-Karger, F. E., Varela, R., Thunell, R., Luerssen, R., Hu, C., and Walsh, J. J. (2005). The importance of continental margins in the global carbon cycle. *Geophysical Research Letters*, 32(1).
- Nash, J. and Sutcliffe, J. (1970). River flow forecasting through conceptual models part i—a discussion of principles. *Journal of hydrology*, 10(3):282–290.
- Ospar, V. M., De Vries, I., Bokhorst, M., Ferreira, J., Gellers-Barkmann, S., Kelly-Gerreyn, B., Lancelot, C., Mensguen, A., Moll, A., Pätsch, J., Radach, G., Skogen, M., Soiland, H., Svendsen, E., and Vested, H. J. (1998). Report of the ASMO modelling workshop on eutrophication Issues, 5–8 November 1996. *OSPAR Commission Report*, 102:90.
- Peterson, R. G. and Stramma, L. (1991). Upper-level circulation in the south atlantic ocean. *Progress in oceanography*, 26(1):1–73.
- Piola, A. and Matano, R. (2001). Brazil and falklands (malvinas) currents. *Ocean Currents: A Derivative of the Encyclopedia of Ocean Sciences*, pages 35–43.

- Piola, A. R., Campos, E. J., Möller, O. O., Charo, M., and Martinez, C. (2000). Subtropical shelf front off eastern south america. *Journal of Geophysical Research: Oceans (1978–2012)*, 105(C3):6565–6578.
- Rippeth, T. P., Lincoln, B. J., Kennedy, H. A., Sharples, J., and Williams, C. A. J. (2014). Impact of vertical mixing on sea surface pCO₂ in temperate seasonally stratified shelf seas. *Journal of Geophysical Research*.
- Sabine, C. L., Hankin, S., Koyuk, H., Bakker, D. C. E., Pfeil, B., Olsen, A., Metzl, N., Kozyr, A., Fassbender, A., Manke, A., Malczyk, J., Akl, J., Alin, S. R., Bellerby, R. G. J., Borges, A., Boutin, J., Brown, P. J., Cai, W.-J., Chavez, F. P., Chen, A., Cosca, C., Feely, R. a., González-Dávila, M., Goyet, C., Hardman-Mountford, N., Heinze, C., Hoppema, M., Hunt, C. W., Hydes, D., Ishii, M., Johannessen, T., Key, R. M., Kötzinger, A., Landschützer, P., Lauvset, S. K., Lefèvre, N., Lenton, A., Lourantou, A., Merlivat, L., Midorikawa, T., Mintrop, L., Miyazaki, C., Murata, A., Nakadate, A., Nakano, Y., Nakaoka, S., Nojiri, Y., Omar, a. M., Padin, X. a., Park, G.-H., Paterson, K., Perez, F. F., Pierrot, D., Poisson, A., Ríos, a. F., Salisbury, J., Santana-Casiano, J. M., Sarma, V. V. S. S., Schlitzer, R., Schneider, B., Schuster, U., Sieger, R., Skjelvan, I., Steinhoff, T., Suzuki, T., Takahashi, T., Tedesco, K., Telszewski, M., Thomas, H., Tilbrook, B., Vandemark, D., Veness, T., Watson, a. J., Weiss, R., Wong, C. S., and Yoshikawa-Inoue, H. (2013). Surface Ocean CO₂ Atlas (SOCAT) gridded data products. *Earth System Science Data*, 5(1):145–153.
- Saraceno, M., D'Onofrio, E., Fiore, M., and Grismeyer, W. (2010). Tide model comparison over the Southwestern Atlantic Shelf. *Continental Shelf Research*, 30(17):1865–1875.
- Sarmiento, J. and Gruber, N. (2006). *Ocean biogeochemical dynamics*. Princeton University Press.
- Sarmiento, J. L., Slater, R., Barber, R., Bopp, L., Doney, S. C., Hirst, A., Kleypas, J., Matear, R., Mikolajewicz, U., Monfray, P., et al. (2004). Response of ocean ecosystems to climate warming. *Global Biogeochemical Cycles*, 18(3).
- Schloss, I. R., Ferreyra, G. A., Ferrario, M. E., Almundoz, G. O., Codina, R., Bianchi, A. A., Ballestrini, C. F., Ochoa, H. A., Pino, D. R., and Poisson, A. (2007). Role of plankton communities in sea-air variations in *pCO₂* in the SW Atlantic Ocean. *MARINE ECOLOGY*, 332:93–106.

- Shchepetkin, A. and McWilliams, J. (2005). The regional oceanic modeling system (ROMS): a split-explicit, free-surface, topography-following-coordinate oceanic model. *Ocean Modelling*, 9(4):347–404.
- Shchepetkin, A. F. and McWilliams, J. C. (2009). Correction and commentary for “ocean forecasting in terrain-following coordinates: Formulation and skill assessment of the regional ocean modeling system” by haidvogel et al., j. comp. phys. 227, pp. 3595–3624. *Journal of Computational Physics*, 228(24):8985–9000.
- Signorini, S. R., Mannino, A., Najjar, R. G., Friedrichs, M. a. M., Cai, W.-J., Salisbury, J., Wang, Z. A., Thomas, H., and Shadwick, E. (2013). Surface ocean p CO₂ seasonality and sea-air CO₂ flux estimates for the North American east coast. *Journal of Geophysical Research: Oceans*, 118(10):5439–5460.
- Takahashi, T., Sutherland, S. C., Sweeney, C., Poisson, A., Metzl, N., Tilbrook, B., Bates, N., Wanninkhof, R., Feely, R. A., Sabine, C., Olafsson, J., and Nojiri, Y. (2002). Global sea–air CO₂ flux based on climatological surface ocean p CO₂, and seasonal biological and temperature effects. *Deep Sea Research Part II: Topical Studies in Oceanography*, 49:1601–1622.
- Takahashi, T., Sutherland, S. C., Wanninkhof, R., Sweeney, C., Feely, R. A., Chipman, D. W., Hales, B., Friederich, G., Chavez, F., Sabine, C., et al. (2009). Climatological mean and decadal change in surface ocean pCO₂, and net sea–air CO₂ flux over the global oceans. *Deep Sea Research Part II: Topical Studies in Oceanography*, 56(8):554–577.
- Thomas, H., Bozec, Y., Elkalay, K., and De Baar, H. J. (2004). Enhanced open ocean storage of CO₂ from shelf sea pumping. *Science*, 304(5673):1005–1008.
- Tsunogai, S., Watanabe, S., and Sato, T. (1999). Is there a “continental shelf pump” for the absorption of atmospheric CO₂? *Tellus B*, 51B:701–712.
- Turi, G., Lachkar, Z., and Gruber, N. (2014). Spatiotemporal variability and drivers of CO₂ and air–sea CO₂ fluxes in the California Current System: an eddy-resolving modeling study. *Biogeosciences*, 11(3):671–690.
- Van Heuven, S., Pierrot, D., Lewis, E., and Wallace, D. (2009). Matlab program developed for CO₂ system calculations. *ORNL/CDIAC-105b. Carbon Dioxide Information Analysis Center, Oak Ridge National Laboratory, US Department of Energy, Oak Ridge, Tennessee*.

- Walsh, J. (1991). Importance of continental margins in the marine biogeochemical cycling of carbon and nitrogen. *Nature*, 350:53–55.
- Wang, A. Z., Cai, W.-J., Wang, Y., and Ji, H. (2005). The southeastern continental shelf of the United States as an atmospheric CO₂ source and an exporter of inorganic carbon to the ocean. *Continental Shelf Research*, 25(16):1917–1941.
- Williams, R. G. and Follows, M. J. (2011). *Ocean dynamics and the carbon cycle: Principles and mechanisms*. Cambridge University Press.
- Yool, A. and Fasham, M. (2001). An examination of the “continental shelf pump” in an open ocean general circulation model. *Global Biogeochemical Cycles*, 15(4):831–844.